

1 **Wearable, epidermal devices for assessment of swallowing function**

2
3 Tarek Rafeedi¹, Abdulhameed Abdal², Beril Polat¹, Katherine A. Hutcheson³, Eileen H. Shinn⁴,
4 Darren J. Lipomi^{1*}

5
6 ¹*Department of NanoEngineering, University of California, San Diego*

7 *9500 Gilman Drive, Mail Code 0448, La Jolla, California 92093-0448, United States*

8
9 ²*Department of Mechanical and Aerospace Engineering, University of California, San Diego*
10 *9500 Gilman Drive, Mail Code 0448, La Jolla, California 92093-0448, United States*

11
12 ³*Department of Head and Neck Surgery, Division of Surgery; Division of Radiation Oncology;*
13 *The University of Texas MD Anderson Cancer Center, Unit 1445, 1515 Holcombe Street, Houston,*
14 *Texas 77030-4009, United States*

15
16 ⁴*Department of Behavioral Sciences, The University of Texas MD Anderson Cancer Center, Unit*
17 *1330, 1155 Pressler Street, Houston, Texas 77230-1439, United States*

18
19 *Author to whom correspondence should be addressed: dlipomi@ucsd.edu

20
21 **Keywords:** swallow monitoring, sallow biomechanics, wearable sensors, materials-enabled
22 sensors, dysphagia, nutrition

23

24

25

26

27

28

29

30

31

32

33

34

35

36

37

38

39

40

41

42

43

1 **Abstract**

2 Swallowing is an ensemble of voluntary and autonomic processes key to maintaining our body's
3 homeostatic balance. Abnormal swallowing (dysphagia) can cause dehydration, malnutrition,
4 aspiration pneumonia, weight loss, anxiety, or even death—especially in older adults—by airway
5 obstruction. To prevent or mitigate these outcomes, it is imperative to regularly assess swallowing
6 ability in those who are at risk of developing dysphagia and those already diagnosed with it.
7 However, current diagnostic tools such as endoscopy, manometry, and videofluoroscopy require
8 access to clinical experts to interpret the results. These results are often sampled from a limited
9 examination timeframe of swallowing activity in a controlled environment. Additionally, there is
10 some risk of periprocedural complications associated with these methods. In contrast, the field of
11 epidermal sensors is finding non-invasive and minimally obtrusive ways to examine swallowing
12 function and dysfunction. In this review, we summarize the current state of wearable devices that
13 are aimed at monitoring swallowing function and detecting its abnormalities. We pay particular
14 attention to the materials and design parameters that enable their operation. We examine a
15 compilation of both proof-of-concept studies (which focus mainly on the engineering of the
16 device) and studies whose aims are biomedical (which may involve larger cohorts of subjects,
17 including patients). Furthermore, we briefly discuss the methods of signal acquisition and device
18 assessment in relevant wearable sensors. Finally, we examine the need to increase adherence and
19 engagement of patients with such devices and discuss enhancements to the design of such
20 epidermal sensors that may encourage greater enthusiasm for at-home and long-term monitoring.

21

22

1 **Main**

2 Swallowing—deglutition—is a physiological process where the muscles of the mouth,
3 throat, and esophagus pass a portion of food or liquid from the oral cavity to the stomach in a
4 coordinated sequence. The process starts with a voluntary initiation and continues with a series of
5 involuntary actions of the muscles.¹ The stages of swallowing and their mechanics are described
6 by paradigmatic models.^{2,3} These models, such as Four Stage (for liquid) and Process Models (for
7 solids), describe the role of relevant anatomical structures chronologically organized by the bolus
8 passage from the oral cavity to the esophagus. In dysphagia (abnormal swallowing) assessment,
9 the models help examine the abnormalities in bolus movement and airway protection to aid in the
10 diagnosis and therapy. Dysphagia can be caused by obstructive and damaged tissue from injury,
11 surgical complications, or muscular damage, especially in old age or myopathic disorders.⁴⁻⁸ It
12 can also be of neurological origins; characterized by impaired control of the peripheral structures
13 that are critical in regulating muscle coordination for swallowing activity.⁹ Reduction in nerve
14 conduction, for instance, may lead to elongated timing of swallowing events.¹⁰⁻¹³ Incidentally, this
15 disease can be caused by or correlated with neurological ailments such as strokes, Parkinson's
16 disease, and dementia, as well as autoimmune disease such as scleroderma.^{5,14,15} The underlying
17 origin of the disease calls for different diagnostic techniques and different courses of treatment. A
18 recent systematic review and meta-analysis showed that the global prevalence of oropharyngeal
19 dysphagia follows an increasing trend.¹⁶ In the United States a 2018 study found that 16.1% of the
20 population described having dysphagia.¹⁷ Other studies suggest that dysphagia occurs in 8-22% of
21 populations over 50 years old, and the number is generally higher for nursing home residents.^{18,19}

1 Although dysphagia can be managed and rehabilitated by interdisciplinary providers
2 including otolaryngologists, gastroenterologists, and speech-language pathologists, it is often a
3 chronic condition requiring lifelong care.^{4,20-22} Procedural and pharmacologic mitigation
4 strategies, as well as a range of exercise maneuvers have been utilized to curb the development
5 and treat this condition.²³⁻³² However, complete recovery from swallowing impairment is often
6 elusive even with successful management.^{33,34} If insufficiently addressed, degraded swallowing
7 function may lead to aspiration pneumonia, weight loss, and anxiety over nutritional intake.³⁵⁻³⁷
8 To diagnose this condition clinicians use tools such as videofluoroscopy,³⁸⁻⁴⁰ endoscopy,⁴¹⁻⁴³ and
9 high-resolution manometry.^{44,45} These tools and procedures are all exclusive to clinical, often
10 specialized, settings, which reduces the access of at-risk populations (e.g., poor, rural, or elderly).
11 Access is further diminished by the cost and the necessity of experienced technicians/clinicians to
12 operate these devices. Additionally, clinical procedures may also cause periprocedural
13 complications, such as pain, injury, and/or anxiety in the case of endoscopy and risks associated
14 with X-ray exposure in the case of video fluoroscopy.⁴⁴ Further, in-clinic screening protocols for
15 swallowing and aspiration such as the Mann Assessment of Swallowing Ability (MASA), Water-
16 Swallow Test (WST), Gugging Swallow Screen (GUSS), and their variations, require the
17 administration and expertise of a trained clinician.⁴⁶⁻⁴⁹

18 Limitations of the current clinical procedures coupled with the opportunities to measure
19 swallowing activity in the natural environment (outside of clinical settings) led researchers to
20 examine different diagnostic tools that are less invasive and unobtrusive. Recent work in skin-
21 interfacing (“epidermal”) electronic devices⁵⁰⁻⁵³ promises to increase access and increase the
22 temporal resolution of measurements (since they can be done between visits to the clinic) with the

1 potential to decrease healthcare costs, inconvenience, and procedural anxiety. Ideally,
2 incorporating advances in nanomaterial-enabled sensors, biomechanics, and machine learning
3 could lead to a role for epidermal devices in the monitoring and rehabilitation of diseases such as
4 dysphagia.

5 In this review, we briefly introduce the physiological structures and biomechanical stages involved
6 in swallowing. After which, we present detailed overview of recent innovations within the field of
7 skin-interfacing wearable sensing modalities utilized for detecting and monitoring swallowing,
8 primarily in the oropharyngeal stages (see **Fig. 1**). Within each sensing modality, we highlight a
9 few of the materials utilized (summarized in **Table 1**) and discuss their functional physical
10 properties. Finally, we probe the challenges and opportunities to transitioning these materials-
11 enabled sensors to an impactful tool for in-clinic and out of clinic (at home) care.

12 **Swallowing Physiology**

13 Physiologically, a swallow is initiated with a voluntary act and sustained with the precise
14 coordination of more than 30 pairs of muscles.^{1,54} The activity recruits different layers of the
15 central nervous system from the cerebral cortex to the medulla oblongata.⁵⁵ Swallowing involves
16 many anatomical structures starting with the oral cavity, pharynx, larynx, and esophagus.^{2,56,57}
17 Along with these structures, other muscles, bones, cartilage, and salivary glands work in
18 coordination to propel the bolus from the oral cavity to the esophagus. Physiologically, swallowing
19 is described differently for liquid and solid boluses. For instance, in describing swallowing liquids,
20 the Four Stage Model is generally used, whereas for swallowing solids, the Process Model may be
21 followed.^{3,58,59}

1 The Four Stage Model as shown in **Fig. 1b** consists of four distinct phases. The first phase
2 is called the oral preparatory stage, and it starts as a bolus is taken into the mouth. The bolus is
3 held on the tongue surface while the anterior and posterior parts of the oral cavity are sealed to
4 prevent leakage into the oropharynx. The tongue propels the bolus from the anterior oral cavity
5 through the posterior into the pharynx in a process known as the oral propulsive stage. The
6 pharyngeal and oral propulsive stages tend to rapidly transition for liquid swallows. In the case of
7 solid boluses, the Process Model delineates the events before the swallow enters the pharyngeal
8 stage.^{2,60} After ingestion of the solid, stage transport occurs when the tongue carries the bolus to
9 the post-canine region onto the lower teeth for chewing. During mastication, cyclic movement of
10 the jaw is established with the coordination of the tongue, cheek, soft-palate, and hyoid bone.^{3,61}
11 As opposed to liquid swallows, the posterior oral cavity is not thoroughly sealed during this
12 phase.^{62,63} Although mastication and the motion of solid boluses within the oral cavity are vital to
13 the execution of the swallow, they go beyond the scope of this review as they bring into question
14 oral, dental, and mandibular assessments among other matters.

15 Common to liquids and solids, the pharyngeal stage characterizes the propulsion of the
16 bolus through the pharynx into the esophagus (see **Fig. 1a-b**). Tight air compression results in
17 pressure on the bolus to achieve clearance through the upper aerodigestive tract.⁶⁴ With the
18 elevation of the soft palate and tongue base retraction, the bolus is pushed against the pharyngeal
19 walls and squeezed downstream. To protect the airways, the vocal folds are closed to seal the
20 glottis.^{65,66} The arytenoids tilt forward to contact with the epiglottic base while the hyoid bone and
21 larynx are pulled upward by the contraction of the suprathyroid muscles and thyrohyoid muscles
22 tilting the epiglottis backward. This sequence seals the laryngeal vestibule as the upper esophageal

1 sphincter relaxes and expands to allow the bolus to pass into the esophagus.^{67,68,69} The esophageal
2 stage transits the intake to the lower esophageal sphincter, and eventually into the stomach by
3 peristalsis.

4 **Clinical Diagnostic Tools**

5 Standardized diagnostic tools such as X-ray videofluoroscopy require the patient to
6 swallow a series of radiocontrast agents (e.g., barium sulfate). These agents can have various
7 viscosities and allow for real-time visualization and assessment of swallowing mechanics. Direct
8 visualization supports the assessment of bolus clearance, including abnormalities such as laryngeal
9 penetration/aspiration and residue (see **Fig. 1c**). It is however accompanied by minor risk factors,
10 namely exposure to ionizing radiation, and/or dulling of taste intensity⁷⁰ and rare allergic reactions
11^{71,72} due to exposure to barium. A more quantitative examination of pharyngeal and upper
12 esophageal sphincter functional abnormalities can be done using high-resolution manometry, to
13 measure internal pressures caused by muscular exertions.⁷⁰ This technique uses a manometric
14 catheter containing several circumferential pressure sensors targeting a series of anatomical
15 structures (e.g. from the velopharynx down to the upper esophageal sphincter). These
16 measurements provide localized pressure evaluation and insight into the timing and coordination
17 of the swallow as seen in **Fig. 1d**.⁴⁵ Although it is more quantitative, manometry still requires
18 evaluation by a trained clinician and is minimally invasive by the nature of transnasal insertion of
19 a catheter. In contrast, wearable sensors cannot produce visualizations such as those shown in **Fig.**
20 **1c**, nor capture the internal pressure of manometry; however, they can offer less obtrusive sensing
21 of swallow exertions and correlated respiratory activity.^{64,73–75}

1 Assessment of electromyographic (EMG) activity, superficially or intramuscularly, is
2 currently considered as non- or minimally invasive tool for assessing muscle function or providing
3 biofeedback in swallow disorder therapy.^{76,77} The muscle groups that are frequently probed include
4 the jaw and perioral, submandibular, tongue, laryngeal and pharyngeal, and cricopharyngeal
5 muscle of the upper esophageal sphincter.⁵⁵ The biopotentials activity of the former two groups is
6 measurable by surface electromyography (sEMG), due to their proximity to the skin. Therefore,
7 sEMG has its limitations when targeting deeper muscle groups. The rest are approached with
8 needle EMG electrodes for deeper and localized targeting, either via the skin or endoscopically,
9 which are currently irreplaceable. The potential risks such as hematoma and pain during coughing,
10 and the precision required for placement constrain the applicability of needle electrodes to clinical
11 settings.^{69,78} Although EMG has some clinical applications, it is not typically used in the diagnosis
12 of swallow disorders. The neuromuscular signals extracted from electromyographic activity,
13 however, can help detect swallowing abnormalities especially when combined with orthogonal
14 forms of sensing and adequate data analysis techniques.

15 **Wearable Sensing Modalities for Swallowing Behavior**

16 *Surface Electromyography Electrodes*

17 Biopotential signals are the sum of action potentials fired by excitable cells such as
18 neurons, myocytes, and cardiomyocytes. They are generated from changes in ion concentration
19 through depolarization and repolarization of the cell membrane, manifesting in the extracellular
20 fluid. Skeletal muscle activity generates such signals. Motor nerve pulses cause muscle fibers to
21 discharge creating motor unit action potentials that compose an EMG signal.^{79,80} A differential
22 voltage can be measured from a pair of electrodes to reveal the depolarization and repolarization

1 phases caused by muscle contraction and relaxation. Such signals can be obtained from epidermal
2 electrodes placed over the target muscle(s). The electrodes convert the propagated ionic currents
3 from muscle activity into the electric current at the electrode interface. The collected
4 electrophysiological signal can later be processed to extract frequency and amplitude features for
5 determining the timing, force, and fatigue of the muscle. The capabilities of such epidermal
6 electrodes have been applied to digitalized medical devices for tremor diagnosis, muscle
7 rehabilitation, gait assessment, and detection of bruxism, among other applications.⁸¹⁻⁸⁵

8 To collect these sEMG signals with high quality, strong electrical contact is needed
9 between the electrode and skin. Commercially available Ag/AgCl electrodes use a thick layer of
10 ionic gel to maintain a contact low impedance between the metal electrode and the skin (hence
11 referred to as wet electrodes). Dry electrodes, on the other hand, require direct and intimate contact
12 between the conductor and the skin. For a better understanding of this electrical contact, resistor-
13 capacitor circuit models are used to design and characterize such electrodes. The Cole
14 bioimpedance model is commonly used for the skin, while electrode models depend on their type
15 and geometry.^{86,87} For instance, in a dry electrode, the top layer of the stratum corneum (~800 nm
16 thickness) is considered as the dielectric material quantifying the capacitance (C_{sc}) of the circuit.
17 Whereas in gel electrodes, the double-layer capacitance (C_{DL}) of the electrolyte gel is utilized.⁸⁸
18 **Fig. 2a** shows the skin and electrode interface of typical wet and dry electrodes and the dry
19 electrode equivalent circuit model in **Fig. 2b**. Recent advancements in thin film and compliant
20 conductive materials and geometries have popularized research on dry electrodes producing
21 compact and unobtrusive wearable electrodes.

1 Action potentials propagated from the deep skin layers can attenuate at the top surface of
2 the skin due to the insulative nature of the stratum corneum (mainly consisting of dead
3 corneocytes).⁸⁹ Thus, the electrode-skin interface is crucial in probing these potentials.
4 Conventional electrodes such as silver/silver-chloride (Ag/AgCl) gel are commercially available
5 and widely used for monitoring muscle activity (among other biopotential activity) because of
6 their reversible electrochemical characteristics. Typical electrolyte gel disperses on the human skin
7 to maintain stable electrical properties between the electrode and skin interface. Ionic diffusion
8 between Ag⁺ and Cl⁻ ions within the electrolyte gel promotes reversible reactions on the electrode
9 surface. Low polarization potential within the capacitive interface mitigates signal fluctuation and
10 maintains a low impedance with a high signal-to-noise ratio (SNR). Despite their reversibility,
11 long-term monitoring is hindered by the hydration state of the gel, reducing the consistency of the
12 signal measured. Moreover, the thickness and rigidity of typical Ag/AgCl electrodes (**Fig. 2a**)
13 decrease the expected usability and comfort for continuous monitoring.⁹⁰

14 In swallowing assessment using sEMG, the adequate surface placement of the electrodes
15 on the neck is imperative to capture the pertinent signals while reducing crosstalk from adjacent
16 muscle activity.⁸⁰ Several recommendations have been suggested to monitor either suprathyroid or
17 infrathyroid muscle coordination for swallowing, such as placing the electrode couples a few
18 centimeters laterally to the neck midline.^{79,91} Other placements include aligning the electrodes with
19 the anterior belly muscle fibers^{75,92}. This is located over the gap between thyroid and cricoid
20 cartilages (see **Fig. 1a, e**). Moreover, the submental surface is an area of interest to monitor the
21 suprathyroid muscle group, which affects hyoid excursion and the opening of the upper esophageal
22 sphincter.^{79,93} In these locations, electrodes can experience frequent mechanical stress exerted by

1 swallowing and neck motion, not to mention the effect of perspiration and body heat on their
2 adhesiveness. Therefore, for longer-term wearable monitoring, better compliant and durable
3 electrodes are required for such applications. Electrode placements observed in recent literature
4 on conformal electrode designs for swallowing are summarized in **Fig. 1e (left)**. While all these
5 placements are capable of capturing the occurrence of the swallow, further investigation is needed
6 to understand the effect of placement on dysphagia detection and estimations of bolus volume.
7 Previous studies utilizing sEMG have statistically examined the effects of bolus viscosity, volume,
8 and participant age on muscle activation patterns.^{94,95}

9 The benefits of a conductive medium such as a gel or paste as a junction between the skin
10 and electrode material have led researchers to examine wet electrode materials based on polymer
11 hydrogels. These cross-linked polymer networks retain the electrolyte solution and can be made
12 using biocompatible precursors and rendered mechanically soft and self-adhesive. They can
13 maintain robust contact with biological substrates and maintain signal fidelity without requiring
14 rigid carrier substrates.⁹⁶⁻⁹⁸ Although hydrogel bioelectronics are exceptionally versatile and
15 tunable in properties, dehydration caused by water transport to the environment can influence their
16 long-term performance.^{99,100} Increasing the water retention capacity by varying electrolyte
17 concentration can be achieved by adding salts.^{101,102}

18 The exceptional electrical conductivities of metals like gold and copper are indispensable
19 in integrated wearable sensors.¹⁰³ However, their mechanical stiffness precludes them from
20 conforming and/or adhering to curved anatomical surfaces, hence they require intricate geometric
21 patterning. Serpentine, buckled, or fractal geometries, can deflect incurred mechanical stress to
22 geometric deformation thus increasing the fracture strain of the metal trace (**Fig. 2c** and **2d**).

1 51,92,104,105 To give these electrodes an elastic restoring force, they are fabricated on a thin (~5 μm)
2 layer of elastomer such as polydimethylsiloxane (PDMS). For improved skin adhesion, a
3 bioadhesive backing (such as Silibione) can be added to laminate the electrode on the submental
4 surface.⁹² Thin metal electrode features are generally patterned with photolithography and physical
5 vapor deposition and supported with a polyimide layer to minimize the bending stress. Finally, a
6 reactive ion etch is used to expose the electrode windows. The stretchability of the mesh
7 filamentary serpentine electrode (~30%) geometry (seen in **Fig. 2d**) exceeds the elasticity of the
8 human skin and complements curvilinear boundaries with a radius of curvature of 45 μm . Two of
9 the electrodes in the patch were placed along (and targeted) the anterior belly of the digastric
10 muscle, while the third was used as a ground. The integrated submental ground electrode on the
11 patch showed lower swallow signal amplitudes when compared to the ground placement on the
12 elbow (likely chosen as a control for its distance from the neck), but it showed lower signal
13 sensitivity to head movements. The size restriction imposed by the additive methods of such
14 fabrication procedures reduces the spatial resolution and span of the epidermal sensor, a key factor
15 for more accurate and extensive monitoring.^{53,106} In that regard, subtractive (top-down)
16 fabrications can yield larger sensor patches allowing a host of spatial and temporal analyses using
17 ML and statistical analysis.^{107–109} **Fig. 2 g and h** show the spatial mapping achievable with sEMG
18 electrodes and emphasize the leap in wearability afforded by new fabrication techniques and
19 advancements in materials for epidermal sensing shown in **Fig. 2h**.

20 Most sEMG experiments on swallowing behavior have been performed in a laboratory
21 setting. Typically, the wearable sensor is physically tethered to backend electronics. This setup is
22 undesirable for at-home monitoring. To address this issue, wireless data acquisition devices

1 combined with wearable sensors can transmit raw signals to a computer for processing and
2 analysis. Incidentally, skin-like electrodes inspired by fractal gold nano-membranes¹¹⁰ can
3 incorporate a flexible carbon connector to a wireless transmitter for continuous monitoring with
4 minimal obtrusiveness¹¹¹. Such devices have been employed in a customized biofeedback
5 classification algorithm to engage healthy participants during swallowing experiments. Real-time
6 video game feedback uses the submental muscle activity signal as the controller (thresholds) for a
7 ball bouncing between platforms (**Fig. 2f**). Cohort studies of the customized human-computer
8 interaction gaming technology were further studied with dysphagic exercises for clinical
9 assessment.¹¹²

10 Despite the robust electronic properties of metallic thin films, the mechanical mismatch
11 between the materials and the soft skin can introduce electrode motion artifacts — a consequence
12 of interfacial disparities. Additionally, elemental and alloyed metals offer minimal tunability in
13 mechanical and electronic properties in thin films. To that end, conducting polymers such as
14 poly(ethylene dioxythiophene):poly(styrene sulfonate) (PEDOT:PSS) has gained traction as an
15 alternative bioelectronic material. The electrical conductivity of the polymer arises from the
16 delocalization of electrons along the alternating single and double bonds, known as π -conjugation.
17 Electrodes based on PEDOT:PSS show low interfacial impedances with skin owing to the high
18 volumetric capacitance and mixed ionic and electronic conductivities in an interpenetrated, 3D
19 network of conductive pathways. Although the intrinsic electrical conductivities are lower than
20 metallic counterparts, many doping strategies have been exploited to provide additional paths for
21 charge carriers along the polymer backbone by inducing favorable morphologies.¹¹³ Moreover, it
22 is possible to tune the elastic modulus to match the location on the skin and increase the durability

1 of such polymers with additives and cross-linkers. Additives such as sorbitol, xylitol, Zonyl FS-
2 300, Triton X-100, and ionic liquids are commonly used in the literature.¹¹⁴⁻¹¹⁸ However, these
3 additives have the potential to leech and are not always biocompatible.

4 Copolymerization is an attractive alternative method of plasticization without the need for
5 molecular additives.¹¹⁹ For example, the block copolymer of PEDOT:PSS with poly(ethylene
6 glycol) methyl ether acrylate) (PPEGMEA) augments the stretchability of the intrinsically brittle
7 neat PEDOT:PSS.¹²⁰ By varying the blocks of PEDOT:PSS₍₁₎-*b*-PPEGMEA_(x) from (*x* ∈
8 {1,2, ... 6}), the elastic modulus can be reduced to ~10 MPa, a magnitude lower than commercially
9 available material. A recent study utilized PEDOT:PSS₍₁₎-*b*-PPEGMEA₍₆₎ electrodes placed on the
10 submental region for swallow volume estimation during exercise. It was demonstrated that
11 electrodes were effective for long-term capturing muscle activity despite the bodily motion (Fig.
12 2e).¹²¹

13 Measured impedances tend to decrease with time when suspended on the skin because of
14 the presence of a sweat layer enriched with electrolytes. Based on the capacitive coupling (Fig.
15 2b), the resistance value, R_s, is extracted from sweat ducts found in the skin.⁸⁸ Therefore, the
16 porous structure of PEDOT:PSS allows for the uptake of water, which can reduce the resistance
17 values and perform as a breathable (vapor-permeable) wearable substrate.^{88,122} The solution
18 processability of this polymer makes for facile molding of freestanding sEMG in the desired
19 geometric designs,¹²¹ and the adaptation of conformal and noise filtering geometries (see **Sensing**
20 **Mechanism and Figures of Merit**). Generally, liquid phase processability is an attractive material
21 trait that allows facile and scalable fabrication of stretchable electronics. Such fabrication
22 approaches include spin-casting, spray coating, dip coating, direct ink writing, and stamping,

1 which can generate thin and conformal films on a variety of substrates.^{116,123–126} In cases where the
2 conductive material is being solvated, the concentration of the solution could be varied to modulate
3 the electronic and mechanical properties of the film.¹²⁷ Collectively, the tunable characteristics,
4 sensing abilities, biocompatibility, and processability are unique advantages of conducting
5 polymers.

6 *Ultrasensitive Strain-gauge Wearable Sensors*

7 The mechanical motion of subcutaneous anatomy exerts mechanical loads on the skin
8 typically resulting in bending, stretching, compression, torsion, and wrinkling. This is typically
9 exemplified in the dynamic skin tension in joint motion.^{128–130} Stress generated by bending joints,
10 expanding lungs, contracting muscles, and laryngeal motion among others strain the skin to various
11 extents. Strain gauges placed on the throat and submental region translate the incurred bending or
12 tensile strain, caused by swallow action, to an electrical signal (**Fig. 3a**). Studies implementing
13 this modality have examined skin deformation due to muscle contractility in the
14 submental/submandibular region or the motion of the larynx. The larynx moves by less than 1 cm
15 anteriorly during a swallow generally causing protrusions in the skin.¹³¹ These protrusions are most
16 pronounced near the laryngeal prominence (LP) and cricoid cartilage. As the larynx traverses
17 vertically, its motion can be measured using mechanical sensors (**Fig. 1e (right)**).

18 Strain gauges, among other wearable sensors, are inherently benign and noninvasive.
19 Recent developments in organic and inorganic nanomaterials have led to many methods to render
20 them more unobtrusive, stretchable, and skin-conforming. From applications in electronic skin to
21 heart rate monitoring, strain gauges come in a range of signal outputs, sensitivities, compliances,
22 and scales.^{8,132–135} These mechanisms of strain gauges can be categorized into piezoresistive

1 (geometrically induced effects), piezoelectric, capacitive, and optoelectronic.¹³⁴ Classical resistive
2 strain gauges and flex sensors are often made from patterned rigid metal alloys carried by flexible
3 polymer substrates. The rigidity of the constituent materials makes it difficult to apply conformally
4 to the skin. Organic conductors, carbon-based nanomaterials (graphene, carbon nanotubes (CNT),
5 etc.), and nanoscale particles (nano-spheres, nanowires, nanoislands, etc.) pose a class of
6 stretchable piezoresistive strain gauges, with sensitivities high enough to detect muscle movements
7 with extremely high sensitivities. Forming composites from conductive fillers and skin-compatible
8 polymer hosts or substrates (PDMS, PU, Ecoflex, etc.), is the most common path to making
9 piezoresistive strain gauges and is commonly adopted in literature. The figure of merit that is
10 associated with piezoresistivity is the gauge factor (GF), as defined in **Eq.3** (see **Sensing**
11 **Mechanisms and Figures of Merit**).

12 Carbon-based materials, such as graphene and CNTs are perhaps some of the most utilized
13 in the literature on strain gauges.^{74,90,121,136–139} In one example, Roh et al. reported a three-layer
14 stacked strain sensor made up of single-wall carbon nanotubes (SWCNTs), PEDOT:PSS, and
15 polyurethane (PU) (**Fig. 3b**).¹³⁹ In lower strain regimes, the stretching of the elastomeric matrix
16 increases the distance between conductive particles. As the strain increases, the conductive
17 pathways break. The addition of PU-PEDOT:PSS conductive polymer ensures that during extreme
18 stretching, some conductive pathways are retained, hence increasing the dynamic range. Previous
19 work done by our group, utilizing single-layer graphene/gold nanoisland (Gr/AuNI) strain sensors,
20 has shown that the addition of a plasticized PEDOT:PSS (“dough”) layer (**Fig. 3c**) increased the
21 stretchability of the piezoresistive film from more than 40 fold (2% to 86%).^{90,121}

1 Systems of ultrahigh stretchability can also be made using hydrogels and organogels^{130,138}.
2 For instance, MXene, which is a class of inorganic conductors, nanosheet introduced to gluten
3 networks showed strain ranges of up to 300% with a GF = 3.2.¹⁰⁵ The shape, color, and optical
4 transparency of the resultant sensor are also important factors to consider when dealing with
5 prolonged device use. Hwang et al. report low-density silver nanowires (AgNWs) with
6 PEDOT:PSS/PU to fabricate a strain sensor.¹⁴⁰ This sensor showed high and uniform optical
7 transparency (~75.3%), with stretchability (up to 100%), and sensitivity to strain (GF = 12 for 2%
8 strain). Another example utilizing MXenes is a highly stretchable (~1200%) strain sensor made
9 self-healable using polyvinyl alcohol (PVA) composite hydrogel matrix. This sensor incorporates
10 a Ti₃C₂T_x filler to form electrodes for a capacitive sensor. The sensor achieved a reasonable
11 capacitive GF of (~0.4) and exceptional self-healability after 150 ms while retaining 97.5%
12 capacitance after breakage. Proof-of-concept studies demonstrate the ability of this sensor to
13 measure deformations (**Fig. 3e**) correlated with the four stages of a swallow (**Fig. 1b**).¹⁴¹ The
14 strains caused by a laryngeal rise or muscle contractions are small compared to limb and finger
15 joints, where such sensors are often applied. Hence, large dynamic ranges (e.g., >50%) are
16 generally not required (**Fig. 3f**).⁷⁴ Nevertheless, many of the sensor systems reviewed here have a
17 sufficiently large strain range to capture the motions of the posterior neck, elbow, and knee joints,
18 and face (**Fig. 3g**).^{130,138,142,143}

19 Liquid metal has also been used to generate patterned resistive sensors and circuits.¹⁴⁴ Jeong et al.
20 utilized the wetting properties of reduced liquid metal alloy (GaInSn), to create a wireless patch
21 for remote strain sensing with robust electrical and mechanical performance (**Fig. 3d**).¹⁴⁵ The
22 resistive strain gauge component fabrication was enabled by exploiting the wetting phenomena of

1 GaInSN on micro-patterned gold serpentines. A proof-of-concept demonstration showed the
2 device detecting swallow activity and 10,000 cycles of reversible stretching.

3

4 *Pressure-based Wearable Sensors*

5 Unlike strain sensing, pressure sensors generate a signal when compressed by a net force
6 normal to the skin surface (**Fig. 4a, left panel**). This mode of operation allows these sensors to
7 occupy generally smaller skin areas than strain or sEMG. The applications of wearable pressure
8 sensors can be similar to those seen for strain sensors, but they see larger applications in artificial
9 skins and wearable touch pads.^{146–150} Reported swallow pressure sensors can be parsed into groups
10 by their mechanism of transduction capacitive, optical, piezoelectric, or piezoresistive. The
11 literature reports several permutations of materials for the electrodes and the dielectric media for
12 capacitive sensors. Kou et al. described a wireless system developed around an
13 NH₄HCO₃/Gr/PDMS dielectric sponge capacitor. The sponge dielectric architecture, widely
14 adopted in literature, imparts higher deformability onto the device (see **Signal Acquisition and**
15 **Figures of Merit** section) enhancing its lower detection limit (5 Pa) and lowering its response
16 time.¹⁵¹ The small planar form factor of the sensor allowed for a patch-mounted antenna for
17 wireless and battery-free transmission. This was primarily enabled by the change in resonant
18 frequency (f_{res}) of the inductor-capacitor (LC) circuit when the capacitance (C) varies due to
19 compression ($f_{res} \propto LC^{-1/2}$). Although high in sensitivity elastomer foams tend to be on the
20 order of 1mm in thickness, which can make the device thicker and less skin-conforming. Thinner
21 dielectric materials (~500 nm) have been examined for swallowing applications. Xia et al. applied
22 a monolayer of colloidal microgel (free-radically polymerized N-isopropyl acrylamide (NIPAm),

1 N, N' – methylene bisacrylamide , and acrylic acid (AAc)) that functioned as both a dielectric and
2 an optical sensor (“etalon”), giving the sensor a dual response to pressure change.¹⁵² By utilizing
3 colloidal photonic crystals, swelling and deswelling of the constituent microgel results in a
4 spectrum of optical and capacitive sensitivity to pressure . In this work, ethanol was used to
5 deswell the microgel resulting in a ~130 nm reduction of diameter and a change in optical signal
6 (**Fig. 4b, left panel**). In principle, mechanical pressure exerted during swallowing could compress
7 the microgel to generate a dual response. However, the optical response sensitivity, represented as
8 a shift in the reflectance spectrum, was much lower than that seen in the capacitive aspect of this
9 device. As a proof-of-concept, the change of capacitance was used to differentiate between water
10 volumes (10 – 30 mL) with larger volumes corresponding to higher signal amplitudes (**Fig. 4b,**
11 **right panel**). To that, a simpler optical approach can be generated using fiber optics. For instance,
12 Maeda et al. used a hetero-core fiber optic pressure sensor embedded in a silicone rubber housing
13 and measured the optical loss due pressure induced deforematation.¹⁵³

14 Piezoelectric materials have seen many applications as wearable technologies in general
15 (in ultrasonic and mechanical sensors) and in swallow evaluation in specific, despite their intrinsic
16 rigidity. The use of common piezoelectric polymers such as polyvinylidene fluoride (PVDF) was
17 demonstrated in a paper by Iizuka et al. where a urethane sheet was lined with piezoelectric sensors
18 and placed near the LP.¹⁵⁴ The piezoelectric array captured the upper and lower laryngeal
19 movement during swallowing in healthy subjects. Parameters such as swallowing latency and
20 maximum lowering and rising velocities were characterized (**Fig. 4d**). By fixing the pitch at 3 mm,
21 the velocity can be extracted by measuring the time difference between sensors’ responses.
22 Velocity responses of the laryngeal movement are complementary measurements to subjective

1 evaluation (speech pathologist), as slow velocity is correlated to clinical aspiration. However, the
2 total thickness of the array required the sensor to be placed by hand, which hindered decoupling
3 bending motions along the axis of the laryngeal movement. To address such issues, researchers
4 opt for thinner and unobstructive form factors. A recent example is the work by Natta et al. which
5 featured patterned, ultra-thin, and flexible piezoelectric aluminum nitride (AlN) film mounted on
6 a soft Kapton tape coupled with sticky PDMS-polyethyleneimine (PEIE) to make a sensor with a
7 total thickness of 26 μm .¹⁵⁵ The sensitivity of this device can capture the pressure produced by the
8 bolus passage (up to 50 KPa). Using this sensor, they were able to extract certain important factors
9 from the data such as the duration of the swallowing act, frequency of spontaneous saliva
10 deglutition, and latency (**Fig. 4c**). Specifically, the deglutition wave (upward and downward of the
11 laryngeal movement) is measured from the voltage responses. Ideally, the deglutition wave
12 consists of two peaks resembling the distinct phases of a swallow. The voltage peaks are responses
13 when the laryngeal pushed the sensor during elevation and descent, respectively. Distortion of the
14 deglutition waveform may infer swallowing abnormality. Also, delay in latency during deglutition
15 is common in elderly patients with reduced motor units.¹⁵⁶ These temporal parameters provide
16 complementary clinical insights into swallowing behavior, which can guide the assessment of
17 swallowing abnormality. The authors also highlighted the superiority of AlN non-toxicity,
18 biocompatibility, and superiority over PVDF piezoelectrics which degrade under heat exposure.
19 Finally, wireless Bluetooth technology was utilized to transfer the collected sensor data into a
20 phone application for a proof-of-concept of untethered point-of-care. Moreover, Lee et al.
21 proposed a pressure sensor comprised of ionic polymer-metal composite (IPMC) material for
22 recognizing throat movements during a swallow.¹⁵⁷ Essentially, a pressure applied to the IPMC

1 induces cations and water molecules to move from high to low-stress regions and create a charge
2 distribution while forming a dielectric potential layer. They also utilized a machine learning
3 algorithm, a support vector machine (SVM) model, to calculate the performance of throat
4 movement detection of the sensor in different activities (e.g., coughing, swallowing, and
5 humming). The double peak present in swallow signals increased the precision of the model
6 (~96%) in differentiating it from other throat motions . Although more commonly used in the strain
7 modality, piezoresistivity can also be used to sense pressure exerted by laryngeal motion. Guan et
8 al. used a molybdenum diselenide/multi-walled carbon nanotubes (MoSe₂/MWNTs) composite
9 capped with PDMS and copper foil electrodes on either side. Among the biosensing
10 demonstrations in this work, the authors placed the sensor above the laryngeal prominence of a
11 male subject and observed swallowing signals as a reduction in the resistance of the sensor (**Fig.**
12 **4e**).¹⁵⁸

13 *Acoustic and accelerometric devices*

14 Many of the movements produced by swallowing produce acoustic signals and vibrations
15 that can be detected at the surface of the skin. Thus, wearable devices featuring MEMS
16 accelerometers and acoustic sensors have the potential to advance traditional diagnostic methods
17 based on auscultation (listening).^{159,160} Specifically, laryngeal microphones (laryngophones), have
18 been applied to the assessment of dysphagia.^{161,162} Unlike strain and pressure sensors which
19 deform with muscular and laryngeal motions, vibration and audio signals encompass a larger range
20 of deformation frequencies (from skin motion to audible swallow sounds).^{64,161,162} For instance,
21 Tao et al. utilized a laser-induced graphene film that could generate and detect sounds from the
22 skin.¹⁶³ This acoustic sensor used direct laser writing (450 nm wavelength) on polyimide (PI)

1 substrates to raster porous graphene films.¹⁶⁴ This porous film structure allowed the detection of
2 weak vibrations (such as vocal sounds) permeating the skin through its high degree of
3 piezoresistance. When placed on the throat, this sensor was able to detect the swallowing activity
4 among other physiological and bioacoustic signals (**Fig. 4g**). Examining the placement and signal
5 amplitude of the device, however, indicates that the swallow signal reported is in part due to large
6 scale deformations of the sensor, and not just acoustic vibrations. Significant developments have
7 been made in adapting commercial imbedded circuits, such as MEMS-based inertial measurement
8 units (IMUs), which can output gyroscopic and accelerometric data, into stretchable and skin
9 adhesive platforms (**Fig. 4f**).⁷³ Using buckled metal interconnects and elastomer substrates, IMUs,
10 and microcontrollers can be mounted onto the skin to achieve close mechanical coupling. This
11 coupling enables the system to detect acoustic vibrations (due to breathing, heart activity, and
12 esophageal contraction). Differential measurements between two accelerometer devices were
13 shown to reduce motion artifacts generated from routine day activities.⁶⁴

14 *Multimodal sensors systems*

15 Obtaining distinct data streams is a key factor in producing robust and efficient machine-
16 learning algorithms and statistical models.¹⁶⁵ Multimodal sensors are relatively new in monitoring
17 swallowing behavior. Early studies that have performed large-scale user testing with their sensors
18 generally combine multiple modalities for cross-validation, a common combination is sEMG with
19 strain or pressure measurement (e.g., **Fig. 2e** and **Fig. 3c**).^{105,121,152} Other studies use a single
20 modality of sensing outputting several orthogonal data streams such as mechanical deformation
21 along a different axis or the activation of various muscle groups.^{74,92,141} Another added benefit of
22 having multiple data streams is failure redundancy. In dysphagia assessment and treatment, for

1 instance, the origin of the disorder can affect the applicability of certain modalities. sEMG swallow
2 assessments show lower precision in diagnosing dysphagia arising from neurological disorders.¹⁶⁶
3 Additionally, comorbidities of dysphagia, either from shared etiology or completely unrelated
4 ones, can reduce the efficacy of certain wearable modalities. For example, lymphedema in the
5 neck area, commonly occurring after radiation cancer treatment, can cause the attenuation of
6 biopotential signals and skin deformations in targeted areas.¹⁶⁷ Edema-induced attenuation effect
7 has been observed with electrocardiogram (ECG) signals.¹⁶⁸ Radiation therapy can also injure the
8 skin on the throat resulting in short-term desquamation and a reduction in necessary contact and
9 adhesion.¹⁶⁹ Similarly, injuries and surgical scars can complicate the wearability of such epidermal
10 devices. Further, extreme differences in morphologies associated with obesity or severe weight
11 loss can greatly affect the reliability of the sensor (by signal attenuation or suboptimal
12 placements).^{168,170} Addressing such challenges is critical since nutrition, hydration, and feeding
13 disorders in general, apart from dysphagia, are of interest in swallowing sensors research.
14^{90,121,171,172} Hence, having hybrid systems, containing an ensemble of sensors can help increase
15 the fidelity of analysis, function as a contingency measure for patients with obstructive
16 comorbidities, and increase the applicability to a wider range of users.

17

18 **Sensing Mechanisms and Figures of Merit**

19 Since wearable swallow sensors are still developing, they are yet to stem well-established metrics
20 for evaluating swallows specifically. Even though swallow health and some of its metrics (like
21 speed, posture, and muscular effort) can be evaluated with wearable sensors, there are currently
22 no overarching mathematical descriptions that can summarize the outcome. However, intertwined

1 within each sensing modality discussed in this work, are the mechanisms that enable a sensor to
2 detect and translate the input it receives to its respective signal. Each sensing mechanism can call
3 for a unique data acquisition and analysis technique. Associated with these techniques are derived
4 metrics and figures of merit all of which are discussed in this section.

5 - EMG Biopotential:

6 The EMG signal arises from the depolarization of skeletal muscle fibers. When probed from the
7 surface, the signals ought to contain the firing action of the collective of fibers under the electrodes.
8 This contrasts with the fiber-targeting, yet invasive, approach in needle EMG.⁸⁰ The raw signal
9 output amplitude of EMG is typically 0-10 mV_{pp} with the energy concentrated in the 20 – 500 Hz
10 frequencies.¹⁷³ Knowing the frequency range of EMG allows for the implementation of filters,
11 such as a 10-20 Hz high-pass filter for low-frequency noise and ECG signals and notch filters for
12 powerline interference.¹⁷⁴ These measures serve to improve the signal-to-noise ratio (SNR); a
13 common metric used to quantify signal quality defined as the ratio of signal power P_{signal} to noise
14 power P_{noise} .

$$SNR = \frac{P_{signal}}{P_{noise}} = \left(\frac{A_{signal}}{A_{noise}} \right)^2 ; \text{where } A \text{ is the amplitude} \quad (1)$$

15 The SNR of an sEMG system can give information about the electrode-skin contact and the
16 effectiveness of the electrode placement. Poor electrode-skin contact, as mentioned earlier, can be
17 a source of noise and unwanted motion artifacts, while an incorrect placement of the electrodes
18 can generate interference potentials from unwanted muscular and neural activity.⁸⁰ Concentric
19 electrode geometry has been shown to address some of these issues by localizing the target muscle

1 and creating spatial (Laplacian) filtering effects. The Laplacian filter can be described by the
2 following equation for a bipolar electrode:

$$L_{Bp} = \frac{4}{(2r^2)}(V_o - V_D) \quad (2)$$

3 where L would be the filtered biopotential signal, V_o and V_D are the potentials at the center and the
4 circumference of radius r circle respectively.¹⁷⁵⁻¹⁷⁷

5 - Piezoresistivity:

6 When an external force deforms a piezoresistive material its electrical conductivity changes.
7 Granted that this change is reversible, it can be used to continuously detect deformations. The
8 correlation between strain and resistance can present itself in a linear or nonlinear fashion over the
9 strain range of the material. Since linearity is typically favored for simpler data analysis,
10 researchers favor the linear regimes of the material. Some patterned metal conductors can also be
11 sensitive to strain despite having low intrinsic piezoresistivity. Geometric effects such as
12 elongation or necking (cross-section constriction) imparted by applied stresses, change the overall
13 resistance while maintaining the intrinsic conductivity. The figure of merit describing
14 piezoresistive sensitivity is the gauge factor (GF): the normalized change in resistance ($\Delta R/R_o$)
15 with respect to changes in strain ($\varepsilon = \Delta\ell/\ell_o$). Many devices reported in the literature contain two
16 linear regimes owing to a variation in the conducive pathways. In this case, the sensor is given two
17 GFs, one for each strain regime. For initial resistance and length R_o and ℓ_o respectively:

$$GF = \frac{\Delta R/R_o}{\Delta\ell/\ell_o} \quad (3)$$

1 Resistive strain gauges are amenable to several data acquisition techniques apart from standard
2 Ohmmeter measurements. Classically strain gauges can be probed with Wheatstone bridge
3 circuits.¹⁷⁸ However, bridge circuit configurations can become complex especially when
4 connecting multiple strain sensors to the circuit. Incorrect balancing of the bridge can also pose a
5 challenge, especially for high-sensitivity sensors, ones with varying baseline resistances, and those
6 with a significant temperature coefficient of resistance (TCR). The alternatives include using a
7 constant current into the leads of the sensor and probing the voltage drop occurring across it or
8 using digital multimeters.¹⁷⁹

9 - Capacitive sensitivity:

10 Typically, a capacitor is a charge-storing device that can be visualized as two electrodes separated
11 by a dielectric medium. The amount of charge that it can theoretically store is dependent on the
12 permittivity of the materials (ϵ), the area of the electrodes (A), and the electrode separation (d). A
13 mechanical input into a capacitive sensor can change these variables causing a measurable change
14 in capacitance. In the parallel plate configuration, the dielectric material is usually composed of
15 soft elastomer that compresses to change the electrode proximity. Often, the polymer dielectric is
16 made porous or patterned with microstructure to impart a range of compliance and reduce the
17 viscoelastic effects.^{132,146,180} These measures can work to reduce the latency of the sensor and its
18 hysteresis by virtue of optimizing the viscoelastic properties.¹⁴⁶ Other designs, such as
19 interdigitated capacitive sensors, while they produce the same effect do not necessarily change
20 their inter-electrode distance. They instead rely on variability in the dielectric material structure
21 for a change in the dielectric constant.¹⁸¹

$$C = \frac{\epsilon A}{d} \quad (4)$$

$$i = C \frac{dv}{dt} \quad (5)$$

1 Like the gauge factor of piezoresistive materials, some literature sources define a GF for capacitive
 2 sensors where the numerator denotes $\Delta C/C_o$. However, capacitive sensors are popular in the
 3 pressure modality; hence they undergo compressive forces. In cases where compressive strain is
 4 difficult to quantify due to internal geometric complexity or scale, the sensitivity could be defined
 5 in terms of stress (pressure):

$$S_{capcitive} = \frac{\Delta C/C_o}{\Delta P} = \frac{\Delta C/C_o}{\Delta F/A} \quad (6)$$

6 where ΔC is the change in capacitance due to loading pressure ΔP . The sensitivity figure S can be
 7 defined for any sensing mechanism where there is a defined baseline signal (in this case C_o) and
 8 change the signal change commensurate with the input pressure. If the area on which the force is
 9 exerted is assumed to be constant, the pressure change can be broken down in **Eq. 6**. Capturing
 10 the capacitance signal tends to be a more challenging task when compared with resistance. Most
 11 of the proof-of-concept sensor papers utilize tethered and stationary LCR (inductance, capacitance,
 12 resistance) meters or customized acquisition systems.^{151,152,181,182} However, as mentioned earlier
 13 these sensors can be integrated into wireless, battery-free devices utilizing antennas to create an
 14 LC (inductor-capacitor) circuit whose resonant frequency is a function of capacitance.

15 - Piezoelectricity:

16 Piezoelectric materials have seen many transducer applications in wearable technologies, both as
 17 actuators and sensors. Their ability to intrinsically generate voltage signals from mechanical input

1 omits the need for powering the sensor.¹⁸³ However, depending on the active materials and their
2 size, the output signals will often require significant amplification. The lattice structure of a
3 piezoelectric material determines its response to different mechanical inputs. Like the sensitivity
4 defined for capacitive sensors, sensitivity can be defined for piezoelectric sensors:

$$S_{\text{piezoelectric}} = \frac{\Delta V}{\Delta P} \quad (7)$$

5 The described mechanisms are those associated with flexible and stretchable sensors. These figures
6 of merit can be used to compare different sensors. In research settings, various data acquisition
7 systems are used to probe signal outputs as mentioned earlier. Recent developments of low energy
8 and compact data acquisition systems have allowed for the dispatching of these mechanisms into
9 wireless platforms.^{155,184} Apart from signal clarity, the latency of the signal is also an important
10 factor. The time delay associated with signal transduction can vary with the signal acquisition
11 system, as well as the mechanical response of the sensor material. More mature wearable sensing
12 mechanisms such as accelerometry and audio signal recordings offer robust signal outputs that can
13 be read with and have extensive support from development microcontroller boards (Arduino,
14 Raspberry Pi, STMicroelectronics, etc.), or custom microcontroller boards.

15 **Translation to the Clinic and Home Use**

16 The ultimate goal of the research in the area of wearable biomedical devices is to transition
17 from the clinic to the home. Barriers to adoption are not, of course, limited to devices to assess
18 swallowing function. However, if strategies for increased engagement and usability could be
19 developed in this context, they could be applied to most types of epidermal devices. The ultimate
20 success of such work would leverage nearly two decades of work on devices in flexible and

1 stretchable form factors. To this end, we highlight two areas for continued research: user
2 engagement and compliance, along with wireless telemetry and power.

3 *User Engagement and Compliance*

4 Engagement with devices is a challenge faced even by commercial technologies. Despite
5 robust sales, 50% of fitness trackers are abandoned after 6-12 months of use. For older adults,
6 engagement is worse: 43% of adults 70 and older reported abandoning devices within the first two
7 weeks.^{185,186} Methods to improve engagement possibly include using haptic or visual feedback to
8 relay information on the health of the swallow or indicate its successful or unsuccessful
9 execution.^{64,111,162} A real-time feedback mechanism could also be coupled with swallowing
10 exercise maneuvers, often prescribed to dysphagic patients, to portray success/failure metrics and
11 maintain exercise pace. The stimulation of nerves to elicit tactile sensations by mechanical or
12 electrical cues has been utilized in diverse biomedical applications such as prosthetics,^{187,188}
13 robotic teleoperations,¹⁸⁹ and biomedical assistive technologies.^{190,191} Conventional mechanisms
14 such as those found in handheld devices like eccentric rotating mass motors (ERMs) and magnetic
15 linear resonant actuators (LRAs) are common in wearable technologies.¹⁹² However, their rigid
16 form factors can limit their integration in soft, dynamic, and curvilinear regions of the human body
17 such as the neck.¹⁹³ Alternatively, devices for electrotactile stimulation can be implemented in a
18 flexible or stretchable form factor.^{194,195} These sensations can vary from sustained pressure,
19 prickle, vibration, and itch.¹⁹⁶ In general, electrotactile devices require low power consumption
20 when compared to mechanical actuators,¹⁹⁷ but may suffer from issues such as desensitization of
21 the skin or even pain.¹⁵⁷ Visual feedback of data in real-time (e.g., as a smartphone app) has also

1 been explored as a means of increasing patient engagement, compliance, and adherence, but little
2 such long-term results have been reported for swallowing devices.¹⁹⁸

3 *Wireless Telemetry and Power*

4 Prototypes of wearable devices developed in the laboratory are often tethered to non-
5 portable equipment for analysis of the data. To enable continuous long-term monitoring of
6 dysphagia in a home environment, system-level integration of various electrical components in a
7 miniaturized patch is required.¹⁹⁹ Nevertheless, data processing is not expected to be performed
8 on the wearable itself. Instead, the patch should communicate wirelessly with a personal device
9 (i.e., phone or computer). Many wearable devices have integrated miniaturized electrical
10 components, along with Bluetooth or near-field communication chips, in a stretchable encapsulant.
11^{200,201} For efficient telemetry, it's common for the dimensions of the antenna to be at least one-
12 quarter of the signal wavelength.²⁰² Other innovative modules demonstrate battery-free wireless
13 power and data telemetry at large power densities for further miniaturization with magnetoelectric
14 phenomena.²⁰³ Parametric designs of the magnetoelectric substrate are paramount, as the resonant
15 frequency and output voltage are a function of the thickness.²⁰⁴

16 **Outlook and Conclusion**

17 The development of engaging yet physically unobtrusive epidermal devices has the
18 potential to assist in the detection and treatment of swallowing dysfunction. The convenience and
19 physical wearability of swallowing sensors has been greatly improved by the realization of flexible
20 and stretchable electronic materials, such as elastomer composites, ionic hydrogels, conductive
21 polymers, and patterned metal conductors. Research for such materials and their application to
22 swallowing behavior is creating new modalities for the detection of swallow health (e.g. strain,

1 pressure) and improving well-documented and previously researched ones (e.g. EMG and acoustic
2 signals). Although the sensing mechanisms associated with such transducers are now established,
3 challenges remain from data interpretation and communication to maintaining user engagement
4 beyond single uses and healthcare provider buy-in. While data acquisition and communication
5 may be improved using existing dispatchable controllers, and wireless communication platforms,
6 the rest of the challenges require further investigation. Swallowing and feeding disorders such as
7 dysphagia require long-term monitoring and care, a feat wearable swallowing sensors are yet to
8 demonstrate in human studies, despite the promising robustness of the used materials. To that end,
9 improvements in this area would entail longer-term examinations of durability and efficacy, and
10 large sample size human subject trials. Another vital step to achieving continuous, passive, and
11 mobile data collection, is the evaluation of sensors under non-stationary subject conditions and
12 out-of-lab settings. These investigations can help identify undesirable artifacts coming from the
13 user's body movement to identify appropriate data filters. In tandem, they would shed light on user
14 adherence and engagement during swallowing therapies, a crucial facet in preventing swallowing
15 and feeding disorders. Feedback systems (visual, auditory, and haptic), as discussed, can thereafter
16 be effectively implemented to improve adherence and engagement metrics.

17 **Acknowledgments**

18 This work was supported by the National Science Foundation award CBET-2223566 and
19 a gift from PepsiCo & the Gatorade Sports Sciences Institute. Additional support was provided by
20 the member companies of the Center for Wearable Sensors in the Jacobs School of Engineering at
21 the University of California, San Diego, including Dexcom, Gore, Honda, Huami, Instrumentation
22 Laboratory, Kureha, Merck KGaA, PepsiCo, Roche, Samsung, and Sony. This work was

1 performed in part at the San Diego Nanotechnology Infrastructure (SDNI), a member of the
2 National Nanotechnology Coordinated Infrastructure, which is supported by the National Science
3 Foundation (Grant ECCS-1542148). A.A, acknowledges the support of Kuwait Foundation for the
4 Advancement of Sciences (KFAS). Figures 1a, 2a, 3a were partially generated using BioRender
5 resources.

6 **Competing Interests**

7 The authors declare no competing financial interest.

8 **Author Contributions**

9 The authors' contributions to this review are as follows: **Initial conception:** Beril Polat,
10 Darren Lipomi. **Guidance:** Darren Lipomi, Eileen H. Shinn, Katherine A. Hutcheson.
11 **Literature search and assembly:** Tarek Rafeedi, Beril Polat, Abdulhameed Abdal **Writing:**
12 Tarek Rafeedi, Abdulhameed Abdal, Beril Polat, Darren J. Lipomi **Figures and Table:** Tarek
13 Rafeedi, Beril Polat. **Editing:** Tarek Rafeedi, Darren J. Lipomi, Eileen H. Shinn, Katherine A.
14 Hutcheson, Abdulhameed Abdal.

15

16

17 **Data Availability**

18 All the data are available within the article or available from the authors upon reasonable
19 request.

20 **Competing Interests:**

21 The Authors declare no Competing Financial or Non-Financial Interests

22

1 References

2 1 Bronwyn Jones. *Normal and Abnormal Swallowing: Imaging in Diagnosis and Therapy*.
3 2003 doi:doi.org/10.1007/978-0-387-22434-3.

4 2 Matsuo K, Palmer JB. Anatomy and Physiology of Feeding and Swallowing: Normal and
5 Abnormal. *Phys Med Rehabil Clin N Am* 2008; **19**: 691–707.

6 3 Hiiemae KM, Palmer JB. Food transport and bolus formation during complete feeding
7 sequences on foods of different initial consistency. *Dysphagia* 1999; **14**: 31–42.

8 4 Eisbruch A, Schwartz M, Rasch C, Vineberg K, Damen E, Van As CJ *et al*. Dysphagia
9 and aspiration after chemoradiotherapy for head-and-neck cancer: Which anatomic
10 structures are affected and can they be spared by IMRT? *Int J Radiat Oncol Biol Phys*
11 2004; **60**: 1425–1439.

12 5 Roden DF, Altman KW. Causes of dysphagia among different age groups: A systematic
13 review of the literature. *Otolaryngol Clin North Am* 2013; **46**: 965–987.

14 6 Hutcheson KA, Lewin JS, Barringer DA, Liseck A, Gunn GB, Moore MWS *et al*. Late
15 dysphagia after radiotherapy-based treatment of head and neck cancer. *Cancer* 2012; **118**:
16 5793–5799.

17 7 Garon BR, Sierzant T, Ormiston C. Silent Aspiration. *Journal of Neuroscience Nursing*
18 2009; **41**: 178–185.

19 8 Argov Z, de Visser M. Dysphagia in adult myopathies. *Neuromuscular Disorders* 2021;
20 **31**: 5–20.

21 9 Smithard DG. Dysphagia : A Geriatric Giant ? The Normal Swallow. *iMedPub Journals*
22 2016; **2**: 1–7.

1 10 Leslie P, Carding PN, Wilson JA. Investigation and management of chronic dysphagia. *Br*
2 *Med J*. 2003; **326**: 433–436.

3 11 Humbert IA, Robbins JA. Dysphagia in the Elderly. *Phys Med Rehabil Clin N Am*. 2008;
4 **19**: 853–866.

5 12 Fujishima I, Fujiu-Kurachi M, Arai H, Hyodo M, Kagaya H, Maeda K *et al*. Sarcopenia
6 and dysphagia: Position paper by four professional organizations. *Geriatr Gerontol Int*
7 2019; **19**: 91–97.

8 13 Rofes L, Arreola V, Romea M, Palomera E, Almirall J, Cabré M *et al*. Pathophysiology of
9 oropharyngeal dysphagia in the frail elderly. *Neurogastroenterology and Motility* 2010;
10 **22**. doi:10.1111/j.1365-2982.2010.01521.x.

11 14 Shaik MR, Shaik NA, Mikdashi J. Autoimmune Dysphagia Related to Rheumatologic
12 Disorders: A Focused Review on Diagnosis and Treatment. *Cureus* 2023.
13 doi:10.7759/cureus.41883.

14 15 Stathopoulos P, Dalakas MC. Autoimmune Neurogenic Dysphagia. *Dysphagia* 2022; **37**:
15 473–487.

16 16 Rajati F, Ahmadi N, Naghibzadeh ZA sadat, Kazeminia M. The global prevalence of
17 oropharyngeal dysphagia in different populations: a systematic review and meta-analysis.
18 *J Transl Med* 2022; **20**. doi:10.1186/s12967-022-03380-0.

19 17 Adkins C, Takakura W, Spiegel BMR, Lu M, Vera-Llonch M, Williams J *et al*.
20 Prevalence and Characteristics of Dysphagia Based on a Population-Based Survey. *Clin*
21 *Gastroenterol Hepatol* 2020; **18**: 1970–1979.

1 18 Serrano Cardona L, Muñoz Mata E. Prevalence and risk factors for dysphagia: a U.S.
2 community study. *Early Hum Dev* 2013; **83**: 1–11.

3 19 Park YH, Han HR, Oh BM, Lee J, Park J ae, Yu SJ *et al*. Prevalence and associated
4 factors of dysphagia in nursing home residents. *Geriatr Nurs (Minneap)* 2013; **34**: 212–
5 217.

6 20 Clavé P, Shaker R. Dysphagia: Current reality and scope of the problem. *Nat Rev
7 Gastroenterol Hepatol* 2015; **12**: 259–270.

8 21 Cooper JS, Fu K, Marks J, Silverman S. Late effects of radiation therapy in the head and
9 neck region. *Int J Radiat Oncol Biol Phys* 1995; **31**: 1141–1164.

10 22 Nguyen NP, Moltz CC, Frank C, Vos P, Smith HJ, Karlsson U *et al*. Dysphagia following
11 chemoradiation for locally advanced head and neck cancer. *Annals of Oncology* 2004; **15**:
12 383–388.

13 23 Hutcheson KA, Bhayani MK, Beadle BM, Gold KA, Shinn EH, Lai SY *et al*. Eat and
14 exercise during radiotherapy or chemoradiotherapy for pharyngeal cancers: Use it or lose
15 it. *JAMA Otolaryngol Head Neck Surg* 2013; **139**: 1127–1134.

16 24 Roe JWG, Drinnan MJ, Carding PN, Harrington KJ, Nutting CM. Patient-reported
17 outcomes following parotid-sparing intensity-modulated radiotherapy for head and neck
18 cancer. How important is dysphagia? *Oral Oncol* 2014; **50**: 1182–1187.

19 25 Feng FY, Kim HM, Lyden TH, Haxer MJ, Worden FP, Feng M *et al*. Intensity-modulated
20 chemoradiotherapy aiming to reduce dysphagia in patients with oropharyngeal cancer:
21 Clinical and functional results. *Journal of Clinical Oncology* 2010; **28**: 2732–2738.

1 26 King SN, Dunlap NE, Tennant PA, Pitts T. Pathophysiology of Radiation-Induced
2 Dysphagia in Head and Neck Cancer. *Dysphagia* 2016; **31**: 339–351.

3 27 Burkhead LM, Sapienza CM, Rosenbek JC. Strength-training exercise in dysphagia
4 rehabilitation: Principles, procedures, and directions for future research. *Dysphagia* 2007;
5 **22**: 251–265.

6 28 Lazarus C. Tongue Strength and Exercise in Healthy Individuals and in Head and Neck
7 Cancer Patients. *Semin Speech Lang* 2006; **27**: 260–267.

8 29 Carnaby-Mann G, Crary MA, Schmalfuss I, Amdur R. ‘Pharyngocise’: Randomized
9 controlled trial of preventative exercises to maintain muscle structure and swallowing
10 function during head-and-neck chemoradiotherapy. *Int J Radiat Oncol Biol Phys* 2012;
11 **83**: 210–219.

12 30 Scheerens C, Tack J, Rommel N. Buspirone, a new drug for the management of patients
13 with ineffective esophageal motility? *United European Gastroenterol J* 2015; **3**: 261–265.

14 31 Cheng I, Sasegbon A, Hamdy S. Effects of pharmacological agents for neurogenic
15 oropharyngeal dysphagia: A systematic review and meta-analysis. *Neurogastroenterology
& Motility* 2022; **34**. doi:10.1111/nmo.14220.

17 32 Nakato R, Manabe N, Hanayama K, Kusunoki H, Hata J, Haruma K. Diagnosis and
18 treatments for oropharyngeal dysphagia: effects of capsaicin evaluated by newly
19 developed ultrasonographic method. *Journal of Smooth Muscle Research* 2020; **56**: 46–
20 57.

1 33 Martin-Harris B, McFarland D, Hill EG, Strange CB, Focht KL, Wan Z *et al.* Respiratory-
2 swallow training in patients with head and neck cancer. *Arch Phys Med Rehabil* 2015; **96**:
3 885–893.

4 34 Ciarambino T, Sansone G, Para O, Giordano M. Dysphagia: What we know? a
5 minireview. *Journal of Gerontology and Geriatrics* 2021; **69**: 188–194.

6 35 Høxbroe Michaelsen S, Grønhøj C, Høxbroe Michaelsen J, Friborg J, von Buchwald C.
7 Quality of life in survivors of oropharyngeal cancer: A systematic review and meta-
8 analysis of 1366 patients. *Eur J Cancer* 2017; **78**: 91–102.

9 36 Nguyen NP, Frank C, Moltz CC, Vos P, Smith HJ, Bhamidipati P V. *et al.* Aspiration rate
10 following chemoradiation for head and neck cancer: An underreported occurrence.
11 *Radiotherapy and Oncology* 2006; **80**: 302–306.

12 37 Eisbruch A, Lyden T, Bradford CR, Dawson LA, Haxer MJ, Miller AE *et al.* Objective
13 assessment of swallowing dysfunction and aspiration after radiation concurrent with
14 chemotherapy for head-and-neck cancer. *Int J Radiat Oncol Biol Phys* 2002; **53**: 23–28.

15 38 Palmer JB, Kuhlemeir K V., Tippett DC, Lynch C. A protocol for the videofluorographic
16 swallowing study. *Dysphagia* 1993; **8**: 209–214.

17 39 Logemann JA. Role of the Modified Barium Swallow in Management of Patients with
18 Dysphagia. *Otolaryngology–Head and Neck Surgery* 1997; **116**: 335–338.

19 40 Martin-Harris B, Logemann JA, McMahon S, Schleicher M, Sandidge J. Clinical utility of
20 the modified barium swallow. *Dysphagia* 2000; **15**: 136–141.

21 41 Langmore SE, Kenneth SMA, Olsen N. Fiberoptic endoscopic examination of swallowing
22 safety: A new procedure. *Dysphagia* 1988; **2**: 216–219.

1 42 Badenduck LA, Matthews TW, McDonough A, Dort JC, Wiens K, Kettner R *et al.* Fiber-
2 optic endoscopic evaluation of swallowing to assess swallowing outcomes as a function of
3 head position in a normal population. *Journal of Otolaryngology - Head and Neck Surgery*
4 2014; **43**: 2–7.

5 43 Bastian RW. Videoendoscopic Evaluation of Patients with Dysphagia: An Adjunct to the
6 Modified Barium Swallow. *Otolaryngology-Head and Neck Surgery* 1991; **104**: 339–350.

7 44 Knigge MA, Thibeault S, Mcculloch TM. Implementation of High-resolution Manometry
8 in the Clinical Practice of Speech Language Pathology. 2014; : 2–16.

9 45 Ryu JS, Park D, Kang JY. Application and interpretation of high-resolution manometry
10 for pharyngeal dysphagia. *J Neurogastroenterol Motil* 2015; **21**: 283–287.

11 46 Antonios N, Carnaby-Mann G, Crary M, Miller L, Hubbard H, Hood K *et al.* Analysis of
12 a Physician Tool for Evaluating Dysphagia on an Inpatient Stroke Unit: The Modified
13 Mann Assessment of Swallowing Ability. *Journal of Stroke and Cerebrovascular
14 Diseases* 2010; **19**: 49–57.

15 47 Somasundaram S, Henke C, Neumann-Haefelin T, Isenmann S, Hattingen E, Lorenz MW
16 *et al.* Dysphagia Risk Assessment in Acute Left-Hemispheric Middle Cerebral Artery
17 Stroke. *Cerebrovascular Diseases* 2014; **37**: 217–222.

18 48 Warnecke T, Im S, Kaiser C, Hamacher C, Oelenberg S, Dziewas R. Aspiration and
19 dysphagia screening in acute stroke – the Gugging Swallowing Screen revisited. *Eur J
20 Neurol* 2017; **24**: 594–601.

1 49 Chen P, Chuang C, Leong C, Guo S, Hsin Y. Systematic review and meta-analysis of the
2 diagnostic accuracy of the water swallow test for screening aspiration in stroke patients. *J
3 Adv Nurs* 2016; **72**: 2575–2586.

4 50 Wagner S, Bauer S. Materials for stretchable electronics. *MRS Bull* 2012; **37**: 207–213.

5 51 Kim D-H, Lu N, Ma R, Kim Y-S, Kim R-H, Wang S *et al*. Epidermal Electronics. *Science
6 (1979)* 2011; **333**: 838–843.

7 52 Kaltenbrunner M, Sekitani T, Reeder J, Yokota T, Kuribara K, Tokuhara T *et al*. An ultra-
8 lightweight design for imperceptible plastic electronics. *Nature* 2013; **499**: 458–463.

9 53 Wang Y, Yin L, Bai Y, Liu S, Wang L, Zhou Y *et al*. Electrically compensated, tattoo-like
10 electrodes for epidermal electrophysiology at scale. *Sci Adv* 2020; **6**.
11 doi:10.1126/sciadv.abd0996.

12 54 Shaw SM, Martino R. The normal swallow: Muscular and neurophysiological control.
13 *Otolaryngol Clin North Am* 2013; **46**: 937–956.

14 55 Ertekin C, Aydogdu I. Neurophysiology of swallowing. *Clinical Neurophysiology* 2003;
15 **114**: 2226–2244.

16 56 Logemann JA. *Evaluation and treatment of swallowing disorders*. 2nd ed. PRO-ED:
17 Austin, 1998.

18 57 Dodds WJ, Stewart ET, Logemann JA. Physiology and Radiology of the Normal Oral and
19 Pharyngeal Phases of Swallowing. *American Journal of Roentgenology* 1989; **154**: 953–
20 963.

21 58 Palmer JB, Rudin NJ, Lara G, Crompton AW. Coordination of mastication and
22 swallowing. *Dysphagia* 1992; **7**: 187–200.

1 59 Dua KS, Ren J, Bardan E, Xie P, Shaker R. Coordination of deglutitive glottal function
2 and pharyngeal bolus transit during normal eating. *Gastroenterology* 1997; **112**: 73–83.

3 60 Palmer JB, Crompton AW. Coordination of Mastication and Swallowing. 1992; **200**: 187–
4 200.

5 61 Matsuo K, Hiiemae KM, Palmer JB. Cyclic motion of the soft palate in feeding. *J Dent
6 Res* 2005; **84**: 39–42.

7 62 Buettner A, Beer A, Hannig C, Settles M. Observation of the swallowing process by
8 application of videofluoroscopy and real-time magnetic resonance imaging-consequences
9 for retronasal aroma stimulation. *Chem Senses* 2001; **26**: 1211–1219.

10 63 Palmer JB, Hiiemae KM. Eating and breathing: interactions between respiration and
11 feeding on solid food. *Dysphagia* 2003; **18**: 169–178.

12 64 Kang YJ, Arafa HM, Yoo JY, Kantarcigil C, Kim JT, Jeong H *et al.* Soft skin-interfaced
13 mechano-acoustic sensors for real-time monitoring and patient feedback on respiratory
14 and swallowing biomechanics. *NPJ Digit Med* 2022; **5**. doi:10.1038/s41746-022-00691-w.

15 65 Shaker R, Dodds WJ, Dantas RO, Hogan WJ, Arndorfer RC. Coordination of deglutitive
16 glottic closure with oropharyngeal swallowing. *Gastroenterology* 1990; **98**: 1478–1484.

17 66 Ohmae Y, Logemann JA, Kaiser P, Hanson DG, Kahrilas PJ. Timing of glottic closure
18 during normal swallow. *Head Neck* 1995; **17**: 394–402.

19 67 Logemann JA, Kahrilas PJ, Cheng J, Pauloski BR, Gibbons PJ, Rademaker AW *et al.*
20 Closure mechanisms of laryngeal vestibule during swallow. *American Journal of
21 Physiology-Gastrointestinal and Liver Physiology* 1992; **262**: G338–G344.

1 68 Cook IJ, Dodds WJ, Dantas RO, Massey B, Kern MK, Lang IM *et al.* Opening
2 mechanisms of the human upper esophageal sphincter. *American Journal of Physiology-
3 Gastrointestinal and Liver Physiology* 1989; **257**: G748–G759.

4 69 Ertekin C, Aydogdu I. Electromyography of human cricopharyngeal muscle of the upper
5 esophageal sphincter. *Muscle Nerve* 2002; **26**: 729–739.

6 70 Daniels SK, Easterling CS. Continued Relevance of Videofluoroscopy in the Evaluation
7 of Oropharyngeal Dysphagia. *Curr Radiol Rep* 2017; **5**: 1–9.

8 71 Lo Re G, Vernuccio F, Di Vittorio ML, Scopelliti L, Di Piazza A, Terranova MC *et al.*
9 Swallowing evaluation with videofluoroscopy in the paediatric population. *Acta
10 Otorhinolaryngologica Italica* 2019; **39**: 279–288.

11 72 Bonilha HS, Huda W, Wilmskoetter J, Martin-Harris B, Tipnis S V. Radiation Risks to
12 Adult Patients Undergoing Modified Barium Swallow Studies. *Dysphagia* 2019; **34**: 922–
13 929.

14 73 Lee K, Ni X, Lee JY, Arafa H, Pe DJ, Xu S *et al.* Mechano-acoustic sensing of
15 physiological processes and body motions via a soft wireless device placed at the
16 suprasternal notch. *Nat Biomed Eng* 2020; **4**. doi:10.1038/s41551-019-0480-6.

17 74 Ramírez J, Rodriguez D, Qiao F, Warchall J, Rye J, Aklike E *et al.* Metallic Nanoislands
18 on Graphene for Monitoring Swallowing Activity in Head and Neck Cancer Patients. *ACS
19 Nano* 2018; **12**: 5913–5922.

20 75 Kantarcigil C, Kim MK, Chang T, Craig BA, Smith A, Lee CH *et al.* Validation of a
21 novel wearable electromyography patch for monitoring submental muscle activity during

1 swallowing: A randomized crossover trial. *Journal of Speech, Language, and Hearing*
2 Research 2020; **63**: 3293–3310.

3 76 Steele C. Treating Dysphagia With sEMG Biofeedback. *The ASHA Leader* 2004; **9**: 2–23.

4 77 Crary MA, Carnaby GD, Groher ME, Helseth E. Functional benefits of dysphagia therapy
5 using adjunctive sEMG biofeedback. *Dysphagia* 2004; **19**: 160–164.

6 78 Ertekin C. Electrophysiological Evaluation of Oropharyngeal Dysphagia in Parkinson's
7 Disease. *J Mov Disord* 2014; **7**: 31–56.

8 79 Wheeler KM, Chiara T, Sapienza CM. Surface Electromyographic Activity of the
9 Submental Muscles During Swallow and Expiratory Pressure Threshold Training Tasks.
10 2007; **116**: 108–116.

11 80 Reaz MBI, Hussain MS. Techniques of EMG signal analysis : detection , processing ,
12 classification and applications. 2006; **8**: 11–35.

13 81 Vescio B, Quattrone A, Nisticò R, Crasà M, Quattrone A. Wearable Devices for
14 Assessment of Tremor. *Front Neurol* 2021; **12**: 1–7.

15 82 Iqbal SMA, Mahgoub I, Du E, Leavitt MA, Asghar W. Advances in healthcare wearable
16 devices. *npj Flexible Electronics* 2021; **5**: 1–14.

17 83 Sethi A, Ting J, Allen M, Clark W, Weber D. Advances in motion and electromyography
18 based wearable technology for upper extremity function rehabilitation: A review. *Journal*
19 of *Hand Therapy* 2020; **33**: 180–187.

20 84 Tao W, Liu T, Zheng R, Feng H. Gait analysis using wearable sensors. *Sensors* 2012; **12**:
21 2255–2283.

1 85 Yamaguchi T, Mikami S, Maeda M, Saito T, Nakajima T, Yachida W *et al.* Portable and
2 wearable electromyographic devices for the assessment of sleep bruxism and awake
3 bruxism: A literature review. *Cranio - Journal of Craniomandibular Practice* 2020; **00**:
4 1–9.

5 86 Hary D, Bekey GA, Antonelli DJ. Circuit Models and Simulation Analysis of
6 Electromyographic Signal Sources—I: The Impedance of EMG Electrodes. *IEEE Trans*
7 *Biomed Eng* 1987; **BME-34**: 758.

8 87 Grimnes S, Martinsen ØG. Cole electrical impedance model - A critique and an
9 alternative. *IEEE Trans Biomed Eng* 2005; **52**: 132–135.

10 88 Ferrari LM, Ismailov U, Greco F, Ismailova E, Ismailov U, Ismailova E. Capacitive
11 Coupling of Conducting Polymer Tattoo Electrodes with the Skin. 2021; **2100352**: 1–8.

12 89 Ruzgas T, Nowacka A, Dahi I, Topgaard D, Sparr E, Bjo S *et al.* Skin Membrane
13 Electrical Impedance Properties under the Influence of a Varying Water Gradient. 2013;
14 **104**. doi:10.1016/j.bpj.2013.05.008.

15 90 Polat B, Becerra LL, Hsu PY, Kaipu V, Mercier PP, Cheng CK *et al.* Epidermal Graphene
16 Sensors and Machine Learning for Estimating Swallowed Volume. *ACS Appl Nano Mater*
17 2021; **4**: 8126–8134.

18 91 Dr. Vladimir VF. HYOID MOVEMENT AND SEMG ACTIVITY DURING NORMAL
19 DISCRETE SWALLOWS, MENDELSON MANEUVER, EFFORTFUL SWALLOW
20 AND EXPIRATORY PRESSURE THRESHOLD TASKS IN HEALTHY ADULTS.
21 *Gastronomía ecuatoriana y turismo local* 1967; **1**: 5–24.

1 92 Constantinescu G, Jeong JW, Li X, Scott DK, Jang KI, Chung HJ *et al.* Epidermal
2 electronics for electromyography: An application to swallowing therapy. *Med Eng Phys*
3 2016; **38**: 807–812.

4 93 Kendall KA, Leonard RJ. Hyoid Movement During Swallowing in Older Patients With
5 Dysphagia. 2001 <http://rsb.info.nih.gov/nih-image>,.

6 94 Reimers-Neils L, Logemann J, Larson C. Viscosity effects on EMG activity in normal
7 swallow. *Dysphagia* 1994; **9**: 101–106.

8 95 Ko JY, Kim H, Jang J, Lee JC, Ryu JS. Electromyographic activation patterns during
9 swallowing in older adults. *Sci Rep* 2021; **11**: 1–10.

10 96 Zhang K, Chen X, Xue Y, Lin J, Liang X, Zhang J *et al.* Tough Hydrogel Bioadhesives
11 for Sutureless Wound Sealing , Hemostasis and Biointerfaces.
12 doi:10.1002/adfm.202111465.

13 97 Yang C, Suo Z. Hydrogel iontronics. *Nat Rev Mater* 2018; **3**: 125–142.

14 98 Wang C, Wang H, Wang B, Miyata H, Wang Y, Nayeem MOG *et al.* On-skin paintable
15 biogel for long-term high-fidelity electroencephalogram recording. *Sci Adv* 2022; **8**: 1–12.

16 99 Lee H, Kim C, Sun J. Stretchable Ionics – A Promising Candidate for Upcoming
17 Wearable Devices. 2018; **1704403**: 1–15.

18 100 Yuk H, Lu B, Zhao X. Hydrogel bioelectronics. *Chem Soc Rev* 2019; **48**: 1642–1667.

19 101 Phys A. Transparent hydrogel with enhanced water retention capacity by introducing
20 highly hydratable salt. 2019; **151903**. doi:10.1063/1.4898189.

21 102 Robinson RA. Ionic Hydration and Activity in Electrolyte Solutions. 1948; **70**: 1870–
22 1878.

1 103 Dang W, Vinciguerra V, Lorenzelli L, Dahiya R. Printable stretchable interconnects.

2 2017.

3 104 Rafeedi T, Lipomi DJ. Multiple pathways to stretchable electronics. .

4 105 Kim MK, Kantarcigil C, Kim B, Baruah RK, Maity S, Park Y *et al.* Flexible submental

5 sensor patch with remote monitoring controls for management of oropharyngeal

6 swallowing disorders. *Sci Adv* 2019; **5**: 1–10.

7 106 Yang S, Chen YC, Nicolini L, Pasupathy P, Sacks J, Su B *et al.* ‘Cut-and-Paste’

8 Manufacture of Multiparametric Epidermal Sensor Systems. *Advanced Materials* 2015;

9 **27**: 6423–6430.

10 107 Malvuccio C, Kamavuako EN. Detection of Swallowing Events and Fluid Intake Volume

11 Estimation from Surface Electromyography Signals. *Proceedings - 2020 IEEE EMBS*

12 *Conference on Biomedical Engineering and Sciences, IECBES 2020* 2021; : 245–250.

13 108 Koyama Y, Ohmori N, Momose H, Yamada S ichi, Kurita H. Detection of swallowing

14 disorders with a multiple-channel surface electromyography sensor sheet. *J Dent Sci* 2022.

15 doi:10.1016/j.jds.2021.12.015.

16 109 Zhu M, Yu B, Yang W, Jiang Y, Lu L, Huang Z *et al.* Evaluation of normal swallowing

17 functions by using dynamic high-density surface electromyography maps. *Biomed Eng*

18 *Online* 2017; **16**: 1–18.

19 110 Norton JJS, Lee DS, Lee JW, Lee W, Kwon O, Won P *et al.* Soft, curved electrode

20 systems capable of integration on the auricle as a persistent brain-computer interface. *Proc*

21 *Natl Acad Sci U S A* 2015; **112**: 3920–3925.

1 111 Nicholls B, Ang CS, Efstratiou C, Lee Y, Yeo WH. Swallowing detection for game
2 control: Using skin-like electronics to support people with dysphagia. *2017 IEEE*
3 *International Conference on Pervasive Computing and Communications Workshops,*
4 *PerCom Workshops 2017* 2017; : 413–418.

5 112 Lee Y, Nicholls B, Lee DS, Chen Y, Chun Y. Soft Electronics Enabled Ergonomic
6 Human-Computer Interaction for Swallowing Training. *Nature Publishing Group* 2017; :
7 1–12.

8 113 Shahrin NA, Ahmad Z, Wong Azman A, Fachmi Buys Y, Sarifuddin N. Mechanisms for
9 doped PEDOT:PSS electrical conductivity improvement. *Mater Adv* 2021; **2**: 7118–7138.

10 114 Lipomi DJ, Lee JA, Vosgueritchian M, Tee BC, Bolander JA, Bao Z. Electronic
11 Properties of Transparent Conductive Films of PEDOT:PSS on Stretchable Substrates.
12 2012.

13 115 Wang Y, Zhu C, Pfattner R, Yan H, Jin L, Chen S *et al.* A highly stretchable, transparent,
14 and conductive polymer. *Sci Adv* 2017; **3**: 1–11.

15 116 Li Y, Tanigawa R, Okuzaki H. Soft and flexible PEDOT / PSS films for applications to
16 soft actuators. 2014. doi:10.1088/0964-1726/23/7/074010.

17 117 Teo MY, Kim N, Kee S, Kim BS, Kim G, Hong S *et al.* Highly Stretchable and Highly
18 Conductive PEDOT : PSS / Ionic Liquid Composite Transparent Electrodes for Solution-
19 Processed Stretchable Electronics. 2017. doi:10.1021/acsami.6b11988.

20 118 He H, Zhang L, Guan X, Cheng H, Liu X, Yu S *et al.* Biocompatible Conductive
21 Polymers with High Conductivity and High Stretchability. 2019.
22 doi:10.1021/acsami.9b07325.

1 119 Bates CM, Bates FS. 50th Anniversary Perspective : Block Polymers □ Pure Potential.
2 2017. doi:10.1021/acs.macromol.6b02355.

3 120 Blau R, Chen AX, Polat B, Becerra LL, Runser R, Zamanimeymian B *et al.* Intrinsically
4 Stretchable Block Copolymer Based on PEDOT:PSS for Improved Performance in
5 Bioelectronic Applications. *ACS Appl Mater Interfaces* 2022; **14**: 4823–4835.

6 121 Polat B, Rafeedi T, Becerra L, Chen AX, Chiang K, Kaipu V *et al.* External Measurement
7 of Swallowed Volume During Exercise Enabled by Stretchable Derivatives of
8 PEDOT:PSS, Graphene, Metallic Nanoparticles, and Machine Learning. *Advanced Sensor
9 Research* 2023; **D**: 2200060.

10 122 Miyamoto A, Lee S, Cooray NF, Lee S, Mori M, Matsuhsia N *et al.* Inflammation-free,
11 gas-permeable, lightweight, stretchable on-skin electronics with nanomeshes. *Nat
12 Nanotechnol* 2017; **12**: 907–913.

13 123 Grancarić AM, Jerković I, Koncar V, Cochrane C, Kelly FM, Soulat D *et al.* Conductive
14 polymers for smart textile applications. 2018 doi:10.1177/1528083717699368.

15 124 Esparza GL, Lipomi DJ. Solid-Phase Deposition : Conformal Coverage. 2021.
16 doi:10.1021/acsmaterialslett.1c00213.

17 125 Lipomi DJ, Vosgueritchian M, Tee BCK, Hellstrom SL, Lee JA, Fox CH *et al.* Skin-like
18 pressure and strain sensors based on transparent elastic films of carbon nanotubes. *Nat
19 Nanotechnol* 2011; **6**: 788–792.

20 126 Choudhary K, Chen AX, Pitch GM, Runser R, Urbina A, Dunn TJ *et al.* Comparison of
21 the Mechanical Properties of a Conjugated Polymer Deposited Using Spin Coating ,

1 Interfacial Spreading , Solution Shearing , and Spray Coating. 2021.

2 doi:10.1021/acsami.1c13043.

3 127 Jin Young O, Kim S, Baik HK, Jeong U. Conducting Polymer Dough for Deformable

4 Electronics. *Advanced Materials* 2016; **28**: 4455–4461.

5 128 Wessendorf AM, Newman DJ. Dynamic understanding of human-skin movement and

6 strain-field analysis. *IEEE Trans Biomed Eng* 2012; **59**: 3432–3438.

7 129 Obropta EW, Newman DJ. Skin strain fields at the shoulder joint for mechanical counter

8 pressure space suit development. *IEEE Aerospace Conference Proceedings* 2016; **2016-**

9 **June**: 1–9.

10 130 Xu H, Jiang X, Yang K, Ren J, Zhai Y, Han X *et al*. Conductive and eco-friendly

11 gluten/MXene composite organohydrogels for flexible, adhesive, and low-temperature

12 tolerant epidermal strain sensors. *Colloids Surf A Physicochem Eng Asp* 2022; **636**:

13 128182.

14 131 Hamlet S, Ezzell G, Aref A. Larynx motion associated with swallowing during radiation

15 therapy. *Int J Radiat Oncol Biol Phys* 1994; **28**: 467–470.

16 132 Amjadi M, Kyung KU, Park I, Sitti M. Stretchable, Skin-Mountable, and Wearable Strain

17 Sensors and Their Potential Applications: A Review. *Adv Funct Mater* 2016; **26**: 1678–

18 1698.

19 133 Afsarimanesh N, Nag A, Sarkar S, Sabet GS, Han T, Mukhopadhyay SC. A review on

20 fabrication, characterization and implementation of wearable strain sensors. *Sens*

21 *Actuators A Phys* 2020; **315**: 112355.

1 134 Souri H, Banerjee H, Jusufi A, Radacsi N, Stokes AA, Park I *et al.* Wearable and
2 Stretchable Strain Sensors: Materials, Sensing Mechanisms, and Applications. *Advanced*
3 *Intelligent Systems* 2020; **2**: 2000039.

4 135 Lu Y, Biswas MC, Guo Z, Jeon JW, Wujcik EK. Recent developments in bio-monitoring
5 via advanced polymer nanocomposite-based wearable strain sensors. *Biosens Bioelectron*
6 2019; **123**: 167–177.

7 136 Zhu Y, Hu Y, Zhu P, Zhao T, Liang X, Sun R *et al.* Enhanced oxidation resistance and
8 electrical conductivity copper nanowires-graphene hybrid films for flexible strain sensors.
9 *New Journal of Chemistry* 2017; **41**: 4950–4958.

10 137 Huang Y, Zhao Y, Wang Y, Guo X, Zhang Y, Liu P *et al.* Highly stretchable strain sensor
11 based on polyurethane substrate using hydrogen bond-assisted laminated structure for
12 monitoring of tiny human motions. *Smart Mater Struct* 2018; **27**. doi:10.1088/1361-
13 665X/aaaba0.

14 138 Sun X, Qin Z, Ye L, Zhang H, Yu Q, Wu X *et al.* Carbon nanotubes reinforced hydrogel
15 as flexible strain sensor with high stretchability and mechanically toughness. *Chemical*
16 *Engineering Journal* 2020; **382**: 122832.

17 139 Roh E, Hwang BU, Kim D, Kim BY, Lee NE. Stretchable, Transparent, Ultrasensitive,
18 and Patchable Strain Sensor for Human-Machine Interfaces Comprising a Nanohybrid of
19 Carbon Nanotubes and Conductive Elastomers. *ACS Nano* 2015; **9**: 6252–6261.

20 140 Hwang BU, Lee JH, Trung TQ, Roh E, Kim D II, Kim SW *et al.* Transparent Stretchable
21 Self-Powered Patchable Sensor Platform with Ultrasensitive Recognition of Human
22 Activities. *ACS Nano* 2015; **9**: 8801–8810.

1 141 Zhang J, Wan L, Gao Y, Fang X, Lu T, Pan L *et al.* Highly Stretchable and Self-Healable
2 MXene / Polyvinyl Alcohol Hydrogel Electrode for Wearable Capacitive Electronic Skin.
3 2019; **1900285**: 1–10.

4 142 Zhang SH, Wang FX, Li JJ, Peng HD, Yan JH, Pan GB. Wearable wide-range strain
5 sensors based on ionic liquids and monitoring of human activities. *Sensors (Switzerland)*
6 2017; **17**: 1–10.

7 143 Wang S, Fang Y, He H, Zhang L, Li C, Ouyang J. Wearable Stretchable Dry and Self-
8 Adhesive Strain Sensors with Conformal Contact to Skin for High-Quality Motion
9 Monitoring. *Adv Funct Mater* 2021; **31**. doi:10.1002/adfm.202007495.

10 144 Dickey MD. Stretchable and Soft Electronics using Liquid Metals. *Advanced Materials*
11 2017; **29**: 1–19.

12 145 Jeong YR, Kim J, Xie Z, Xue Y, Won SM, Lee G *et al.* Skin-attachable , stretchable
13 integrated system based on liquid GaInSn for wireless human motion monitoring with
14 multi-site sensing capabilities. *Nature Publishing Group* 2017; : 1–8.

15 146 Pan H, Lee TW. Recent Progress in Development of Wearable Pressure Sensors Derived
16 from Biological Materials. *Adv Healthc Mater* 2021; **10**: 1–17.

17 147 Wang H, Li Z, Liu Z, Fu J, Shan T, Yang X *et al.* Flexible capacitive pressure sensors for
18 wearable electronics. *J Mater Chem C Mater* 2022; **10**: 1594–1605.

19 148 Chen W, Yan X. Progress in achieving high-performance piezoresistive and capacitive
20 flexible pressure sensors: A review. *J Mater Sci Technol* 2020; **43**: 175–188.

1 149 He J, Zhang Y, Zhou R, Meng L, Pan C, Mai W *et al.* Recent advances of wearable and
2 flexible piezoresistivity pressure sensor devices and its future prospects. *Journal of*
3 *Materomics* 2020; **6**: 86–101.

4 150 Li R, Zhou Q, Bi Y, Cao S, Xia X, Yang A *et al.* Research progress of flexible capacitive
5 pressure sensor for sensitivity enhancement approaches. *Sens Actuators A Phys* 2021; **321**:
6 112425.

7 151 Kou H, Zhang L, Tan Q, Liu G, Dong H, Zhang W *et al.* Wireless wide-range pressure
8 sensor based on graphene/PDMS sponge for tactile monitoring. *Sci Rep* 2019; **9**: 1–7.

9 152 Xia X, Zhang X, Serpe MJ, Zhang Q. Microgel-Based Devices as Wearable Capacitive
10 Electronic Skins for Monitoring Cardiovascular Risks. *Adv Mater Technol* 2020; **5**: 1–8.

11 153 Maeda M, Kadokura M, Aoki R, Kawakami M, Koyama Y, Nishiyama M *et al.* Non-
12 invasive swallowing examination device using hetero-core fiber optic pressure sensor.
13 *LifeTech 2021 - 2021 IEEE 3rd Global Conference on Life Sciences and Technologies*
14 2021; : 315–316.

15 154 Iizuka M, Kobayashi M, Hasegawa Y, Tomita K, Takeshima R, Izumizaki M. A new
16 flexible piezoelectric pressure sensor array for the noninvasive detection of laryngeal
17 movement during swallowing. *Journal of Physiological Sciences* 2018; **68**: 837–846.

18 155 Natta L, Guido F, Algieri L, Mastronardi VM, Rizzi F, Scarpa E *et al.* Conformable AlN
19 Piezoelectric Sensors as a Non-invasive Approach for Swallowing Disorder Assessment.
20 *ACS Sens* 2021; **6**: 1761–1769.

21 156 Namasivayam-MacDonald AM, Barbon CEA, Steele CM. A review of swallow timing in
22 the elderly. *Physiol Behav* 2018; **184**: 12–26.

1 157 Lee JH, Chee PS, Lim EH, Tan CH. Artificial intelligence-assisted throat sensor using
2 ionic polymer–metal composite (IPMC) material. *Polymers (Basel)* 2021; **13**.
3 doi:10.3390/polym13183041.

4 158 Guan J, Zhang D, Li T. Flexible Pressure Sensor Based on Molybdenum Diselide/Multi-
5 Walled Carbon Nanotubes for Human Motion Detection. *IEEE Sens J* 2021; **21**: 10491–
6 10497.

7 159 Hu Y, Kim EG, Cao G, Liu S, Xu Y. Physiological Acoustic Sensing Based on
8 Accelerometers: A Survey for Mobile Healthcare. *Ann Biomed Eng* 2014; **42**: 2264–2277.

9 160 Dudik JM, Jestrović I, Luan B, Coyle JL, Sejdić E. A comparative analysis of swallowing
10 accelerometry and sounds during saliva swallows. *Biomed Eng Online* 2015; **14**: 1–15.

11 161 Khalifa Y, Coyle JL, Sejdić E. Non-invasive identification of swallows via deep learning
12 in high resolution cervical auscultation recordings. *Sci Rep* 2020; **10**: 1–13.

13 162 Kuramoto N, Ichimura K, Jayatilake D, Shimokakimoto T, Hidaka K, Suzuki K. Deep
14 Learning-Based Swallowing Monitor for Realtime Detection of Swallow Duration.
15 *Proceedings of the Annual International Conference of the IEEE Engineering in Medicine
16 and Biology Society, EMBS* 2020; **2020-July**: 4365–4368.

17 163 Tao LQ, Tian H, Liu Y, Ju ZY, Pang Y, Chen YQ *et al.* An intelligent artificial throat with
18 sound-sensing ability based on laser induced graphene. *Nat Commun* 2017; **8**: 1–8.

19 164 Lin J, Peng Z, Liu Y, Ruiz-Zepeda F, Ye R, Samuel ELG *et al.* Laser-induced porous
20 graphene films from commercial polymers. *Nat Commun* 2014; **5**: 5–12.

21 165 Cai J, Luo J, Wang S, Yang S. Feature selection in machine learning: A new perspective.
22 *Neurocomputing* 2018; **300**: 70–79.

1 166 Vaiman M, Eviatar E. Surface electromyography as a screening method for evaluation of
2 dysphagia and odynophagia. *Head Face Med* 2009; **5**: 9.

3 167 Ridner SH, Dietrich MS, Niermann K, Cmelak A, Mannion K, Murphy B. A Prospective
4 Study of the Lymphedema and Fibrosis Continuum in Patients with Head and Neck
5 Cancer. *Lymphat Res Biol* 2016; **14**: 198–205.

6 168 Macfarlane PW, van Oosterom A, Pahlm O, Kligfield P, Janse M, Camm J (eds.).
7 *Comprehensive Electrocardiology*. Springer London: London, 2010 doi:10.1007/978-1-
8 84882-046-3.

9 169 Hymes SR, Strom EA, Fife C. Radiation dermatitis: Clinical presentation,
10 pathophysiology, and treatment 2006. *J Am Acad Dermatol* 2006; **54**: 28–46.

11 170 Kuiken* TA, Lowery MM, Stoykov NS. The effect of subcutaneous fat on myoelectric
12 signal amplitude and cross-talk. 2003.

13 171 Selamat NA, Ali SHMd. Automatic Food Intake Monitoring Based on Chewing Activity:
14 A Survey. *IEEE Access* 2020; **8**: 48846–48869.

15 172 Kalantarian H, Alshurafa N, Le T, Sarrafzadeh M. Monitoring eating habits using a
16 piezoelectric sensor-based necklace. *Comput Biol Med* 2015; **58**: 46–55.

17 173 Chu JU, Moon I, Lee YJ, Kim SK, Mun MS. A supervised feature-projection-based real-
18 time EMG pattern recognition for multifunction myoelectric hand control. *IEEE/ASME
19 Transactions on Mechatronics* 2007; **12**: 282–290.

20 174 E. A. Clancy, E. L. Morin, R Merletti. Sampling, noise-reduction and amplitude
21 estimation issues in surface electromyography. *Ophthalmologe* 2016; **113**: 933–942.

1 175 Besio G, Koka K, Aakula R, Weizhong Dai. Tri-polar concentric ring electrode
2 development for Laplacian electroencephalography. *IEEE Trans Biomed Eng* 2006; **53**:
3 926–933.

4 176 Wang K, Parekh U, Pailla T, Garudadri H, Gilja V, Ng TN. Stretchable Dry Electrodes
5 with Concentric Ring Geometry for Enhancing Spatial Resolution in Electrophysiology.
6 *Adv Healthc Mater* 2017; **6**. doi:10.1002/adhm.201700552.

7 177 Garcia-Casado J, Prats-Boluda G, Ye-Lin Y, Restrepo-Agudelo S, Perez-Giraldo E,
8 Orozco-Duque A. Evaluation of Swallowing Related Muscle Activity by Means of
9 Concentric Ring Electrodes. *Sensors* 2020; **20**: 5267.

10 178 Park J, You I, Shin S, Jeong U. Material Approaches to Stretchable Strain Sensors.
11 *ChemPhysChem* 2015; **16**: 1155–1163.

12 179 Issam Abu-Mahfouz. *Instrumentation: Theory and Practice, Part 2: Sensors and
13 Transducers*. Springer Nature Switzerland AG, 2022.

14 180 Homayounfar SZ, Andrew TL. Wearable Sensors for Monitoring Human Motion: A
15 Review on Mechanisms, Materials, and Challenges. *SLAS Technol* 2020; **25**: 9–24.

16 181 Qin R, Hu M, Li X, Liang T, Tan H, Liu J *et al*. A new strategy for the fabrication of a
17 flexible and highly sensitive capacitive pressure sensor. *Microsyst Nanoeng* 2021; **7**: 1–
18 12.

19 182 Ma Z, Zhang Y, Zhang K, Deng H, Fu Q. Recent progress in flexible capacitive sensors:
20 Structures and properties. *Nano Materials Science* 2022.
21 doi:10.1016/j.nanoms.2021.11.002.

1 183 Wang Y, Yu Y, Wei X, Narita F. Self-Powered Wearable Piezoelectric Monitoring of
2 Human Motion and Physiological Signals for the Postpandemic Era: A Review. *Adv
3 Mater Technol* 2022; **7**: 2200318.

4 184 Park DY, Joe DJ, Kim DH, Park H, Han JH, Jeong CK *et al.* Self-Powered Real-Time
5 Arterial Pulse Monitoring Using Ultrathin Epidermal Piezoelectric Sensors. *Advanced
6 Materials* 2017; **29**. doi:10.1002/adma.201702308.

7 185 Ledger Dan, McCaffrey D. Inside Wearables Part 1: How behavior change unlocks long-
8 term engagement. 2014.

9 186 Hermsen S, Moons J, Kerkhof P, Wiekens C, De Groot M. Determinants for Sustained
10 Use of an Activity Tracker: Observational Study. *JMIR Mhealth Uhealth* 2017; **5**: e164.

11 187 Jung YH, Yoo J-Y, Vázquez-Guardado A, Kim J-H, Kim J-T, Luan H *et al.* A wireless
12 haptic interface for programmable patterns of touch across large areas of the skin. *Nat
13 Electron* 2022; **5**: 374–385.

14 188 Schweisfurth MA, Markovic M, Dosen S, Teich F, Graimann B, Farina D. Electrotactile
15 EMG feedback improves the control of prosthesis grasping force. *J Neural Eng* 2016; **13**:
16 056010.

17 189 Keef C V., Kayser L V., Tronboll S, Carpenter CW, Root NB, Finn M *et al.* Virtual
18 Texture Generated Using Elastomeric Conductive Block Copolymer in a Wireless
19 Multimodal Haptic Glove. *Advanced Intelligent Systems* 2020; **2**: 2000018.

20 190 Lin W, Zhang D, Lee WW, Li X, Hong Y, Pan Q *et al.* Super-resolution wearable
21 electrotactile rendering system. *Sci Adv* 2022; **8**. doi:10.1126/sciadv.abp8738.

1 191 Li Z, Ma Y, Zhang K, Wan J, Zhao D, Pi Y *et al.* Air Permeable Vibrotactile Actuators for
2 Wearable Wireless Haptics. *Adv Funct Mater* 2023; **33**: 2211146.

3 192 Yin J, Hinchet R, Shea H, Majidi C. Wearable Soft Technologies for Haptic Sensing and
4 Feedback. *Adv Funct Mater* 2021; **31**: 2007428.

5 193 Yu X, Xie Z, Yu Y, Lee J, Vazquez-Guardado A, Luan H *et al.* Skin-integrated wireless
6 haptic interfaces for virtual and augmented reality. *Nature* 2019; **575**: 473–479.

7 194 Moroni M, Servin-Vences MR, Fleischer R, Sánchez-Carranza O, Lewin GR.
8 Voltage gating of mechanosensitive PIEZO channels. *Nat Commun* 2018; **9**: 1096.

9 195 McNeal DR. Analysis of a Model for Excitation of Myelinated Nerve. *IEEE Trans
10 Biomed Eng* 1976; **BME-23**: 329–337.

11 196 Kajimoto H, Kawakami N, Tachi S, Inami M. SmartTouch: electric skin to touch the
12 untouchable. *IEEE Comput Graph Appl* 2004; **24**: 36–43.

13 197 Kourtesis P, Argelaguet F, Vizcay S, Marchal M, Pacchierotti C. Electrotactile Feedback
14 Applications for Hand and Arm Interactions: A Systematic Review, Meta-Analysis, and
15 Future Directions. *IEEE Trans Haptics* 2022; **15**: 479–496.

16 198 Zhu J, Wang X, Chen S, Du R, Zhang H, Zhang M *et al.* Improving compliance with
17 swallowing exercise to decrease radiotherapy-related dysphagia in patients with head and
18 neck cancer. *Asia Pac J Oncol Nurs* 2023; **10**: 100169.

19 199 O'Brien MK, Botonis OK, Larkin E, Carpenter J, Martin-Harris B, Maronati R *et al.*
20 Advanced Machine Learning Tools to Monitor Biomarkers of Dysphagia: A Wearable
21 Sensor Proof-of-Concept Study. *Digit Biomark* 2021; **5**: 167–175.

1 200 Liu S, Rao Y, Jang H, Tan P, Lu N. Strategies for body-conformable electronics. *Matter*
2 2022; **5**: 1104–1136.

3 201 Yang Y, Wu M, Vázquez-Guardado A, Wegener AJ, Grajales-Reyes JG, Deng Y *et al.*
4 Wireless multilateral devices for optogenetic studies of individual and social behaviors.
5 *Nat Neurosci* 2021; **24**: 1035–1045.

6 202 Nan K, Feig VR, Ying B, Howarth JG, Kang Z, Yang Y *et al.* Mucosa-interfacing
7 electronics. *Nat Rev Mater* 2022; **7**: 908–925.

8 203 Chen JC, Kan P, Yu Z, Alrashdan F, Garcia R, Singer A *et al.* A wireless millimetric
9 magnetoelectric implant for the endovascular stimulation of peripheral nerves. *Nat*
10 *Biomed Eng* 2022; **6**: 706–716.

11 204 Sayeed SYB, Abdal A, Gaire P, Bhardwaj S, Sorushiani S, Volakis J *et al.* Chipscale
12 Piezo-Magnetostrictive Interfaces - A new simplified and microminiaturized telemetry
13 paradigm for Medical Device Packages. In: *2021 IEEE 71st Electronic Components and*
14 *Technology Conference (ECTC)*. IEEE, 2021, pp 1219–1225.

15

16

17

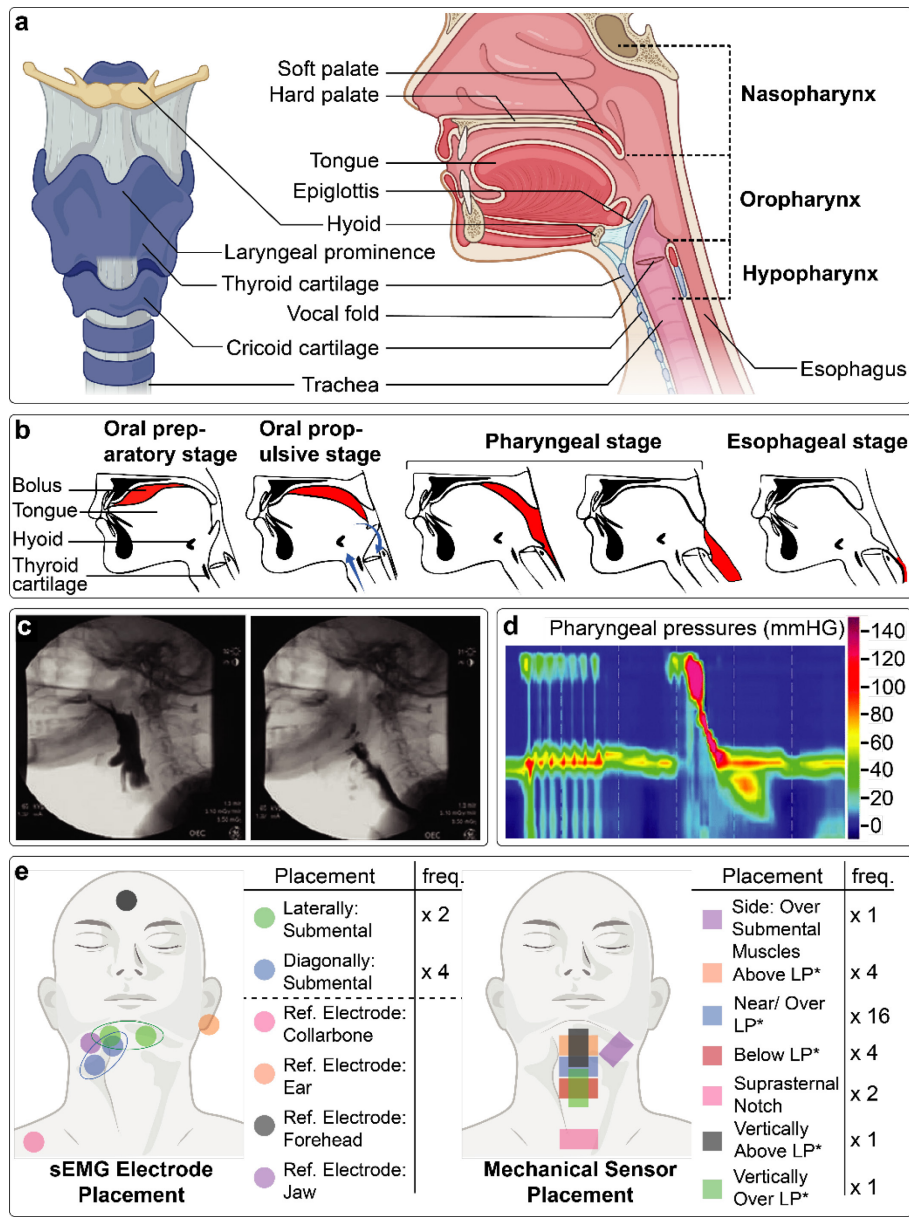
18

19

20

21

22



1

2

3

Figure 1: Illustrates the physiology and anatomy relevant to swallowing and its characterization. **a**, Depicts a sagittal cross-section of the oral to upper esophageal anatomy of the digestive tract (*right*) and a frontal plane depiction of the larynx (*left*) highlighting relevant anatomies. **b**, Is a recreated figure showing the phases of the Four Stage Model for liquid swallowing (arrows were added to depict larynx and epiglottis motion). **c**, Images of dysphagic videofluoroscopy swallows showing penetration into the vocal folds (*left*) and aspiration (*right*). **d**, A graphical representation of high-resolution manometry results with initial velopharyngeal vocalizations where the horizontal axis is time, vertical is relative location, and color scheme represents pressure. **e**, A schematic depicting the visually examined placement of materials-enabled sEMG sensing electrodes (*left*) and proximal placements of reference electrode, and mechanical sensors (*right*) with flexible or stretchable characteristics used in recent literature. The number of electrodes/sensors with similar placement (freq.) is shown in the tables adjacent to each panel. *Note LP: *Laryngeal prominence*. Panel **b** and **c** reproduced with permission.^{2,70}

1

2

3

4

5

6

7

8

9

10

11

12

13

14

15

16

17

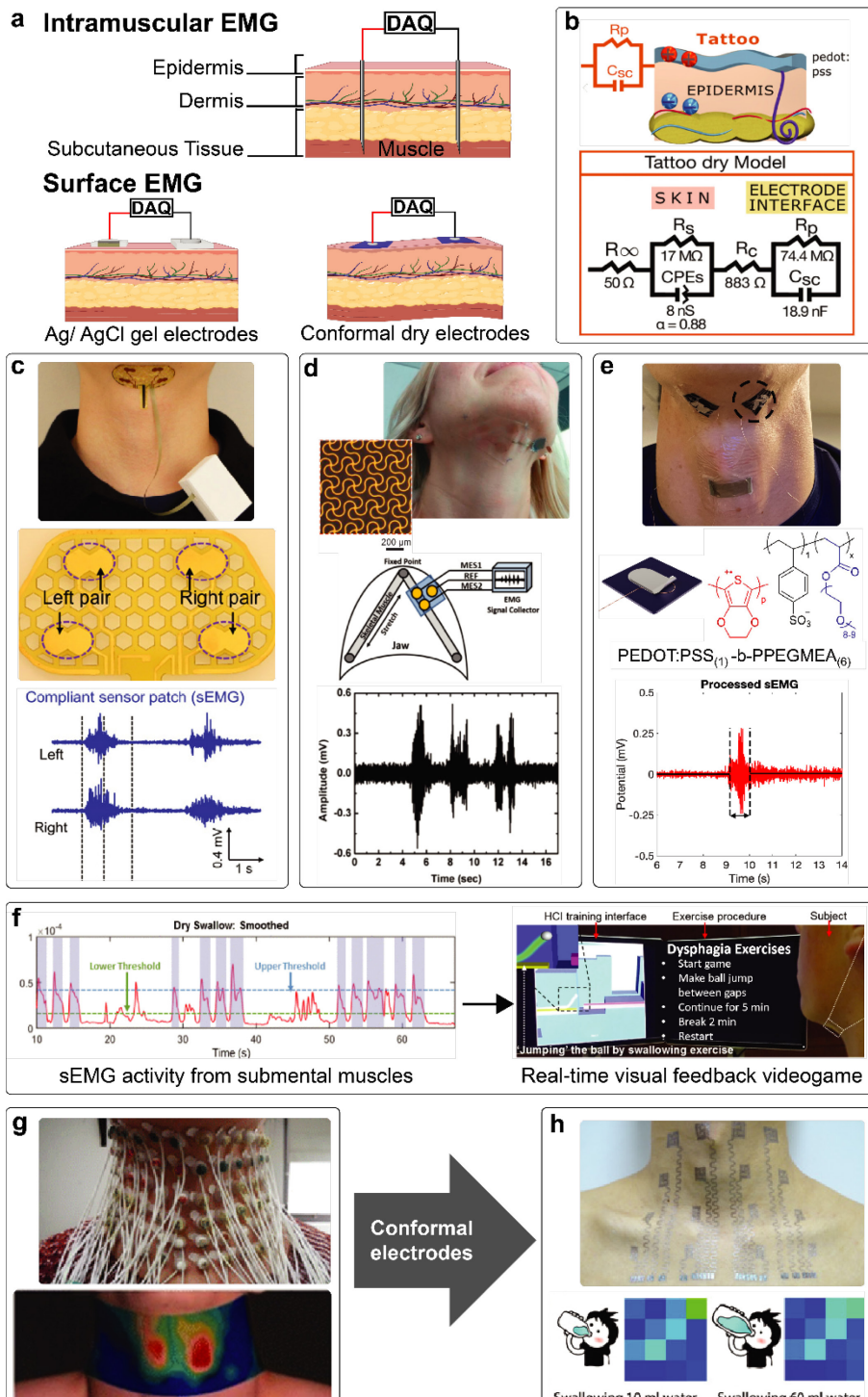
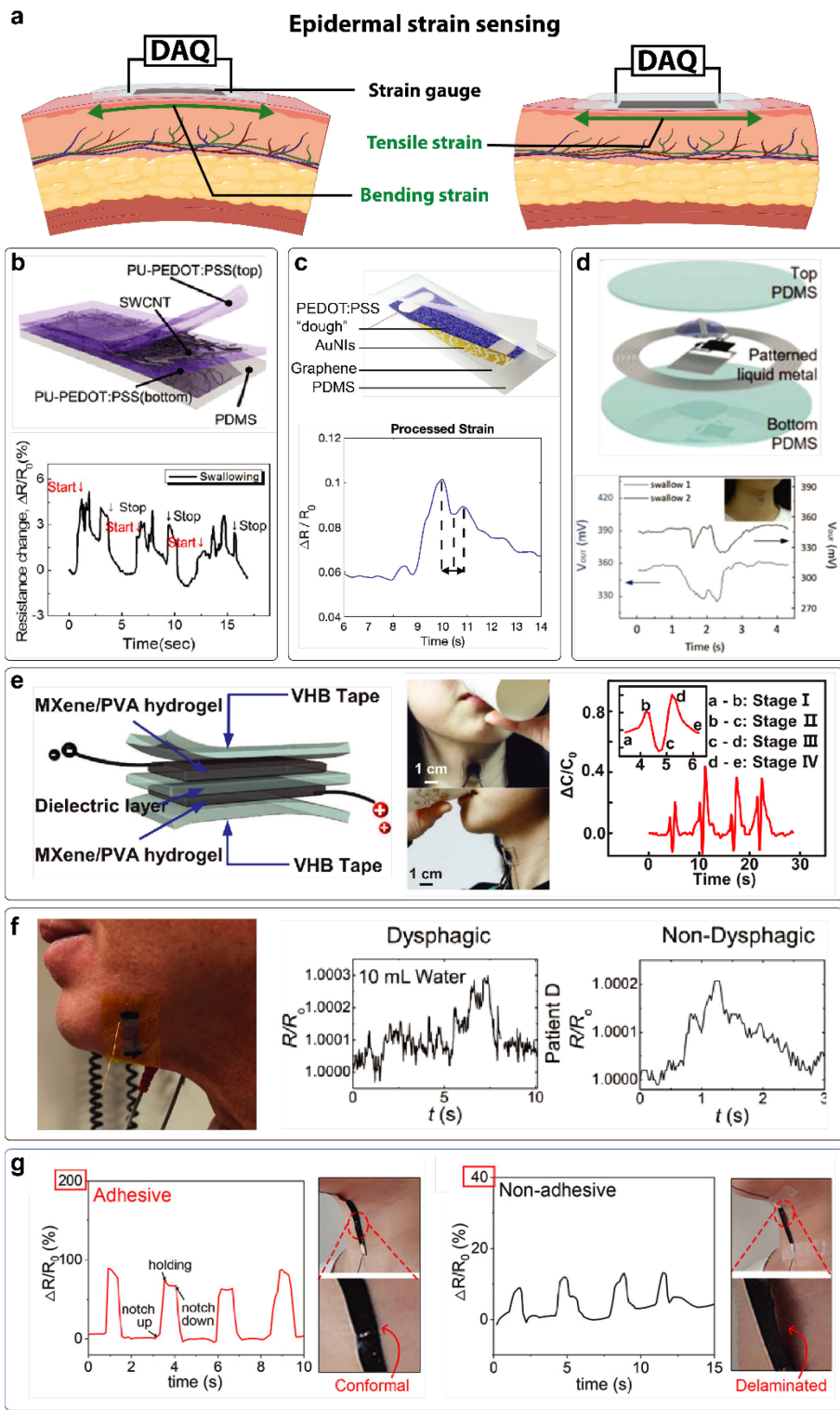


Figure 2: Overview of conformal electromyography electrodes applied to swallowing tests. **a**, A comparative schematic of EMG electrode types: Intramuscular (needle) EMG, gel sEMG electrodes, and conformal electrodes (in this case resembling dry polymer electrodes). **b**, Equivalent circuit model of polymer-based (PEDOT:PSS) sEMG electrodes on skin. **c – e**, Epidermal conformal electrodes with their respective placements, sensor geometry, and sample outputs for the shown placement. **f**, Shows the electromyographic data from submental muscles and the application of the electrodes in a swallowing exercise game. **g, h**, Multichannel array of sEMG electrodes for swallowing mapping showing the contrast between the obstructive system based on classical electrodes in **g** and the thin epidermal patch in **h**. Both figure boxes demonstrate the output biopotential map during select stages of the swallow. Panels **b, d**, reproduced with permission.^{88,92} Panels **c, e-h**, reproduced under Creative Commons (CC BY) license.^{53,105,109,112,121}

1
2
3
4
5
6
7
8
9
10
11
12
13
14
15
16
17



1

2

Figure 3: Overview of materials-based wearable strain gauges applied in swallowing examination. **a**, Epidermal strain sensors reacting to typical skin bending and tensile strains with the appropriate data acquisition systems connected to them. **b – d**, Example strain gauge schematics showing active materials and encapsulants with a sample swallow strain signal respectively. **e**, PVA/ MXene-based capacitive sensor with sample signal expressing laryngeal motion in four stages. **f**, Submental swallow activity monitoring using a palladium nanoislands on graphene sensor, comparing dysphagic and non-dysphagic signal outcomes. **g**, Comparative pictures, and corresponding plots demonstrating the effect of conformal adhesion on strain gauge response. Panels **b, e, f, g**, reproduced with permission.^{74,139,141,143} Panels **c, d**, reproduced under Creative Commons (CC BY) license.^{121,145}

1
2
3
4
5
6
7
8
9
10
11
12
13
14
15
16
17
18

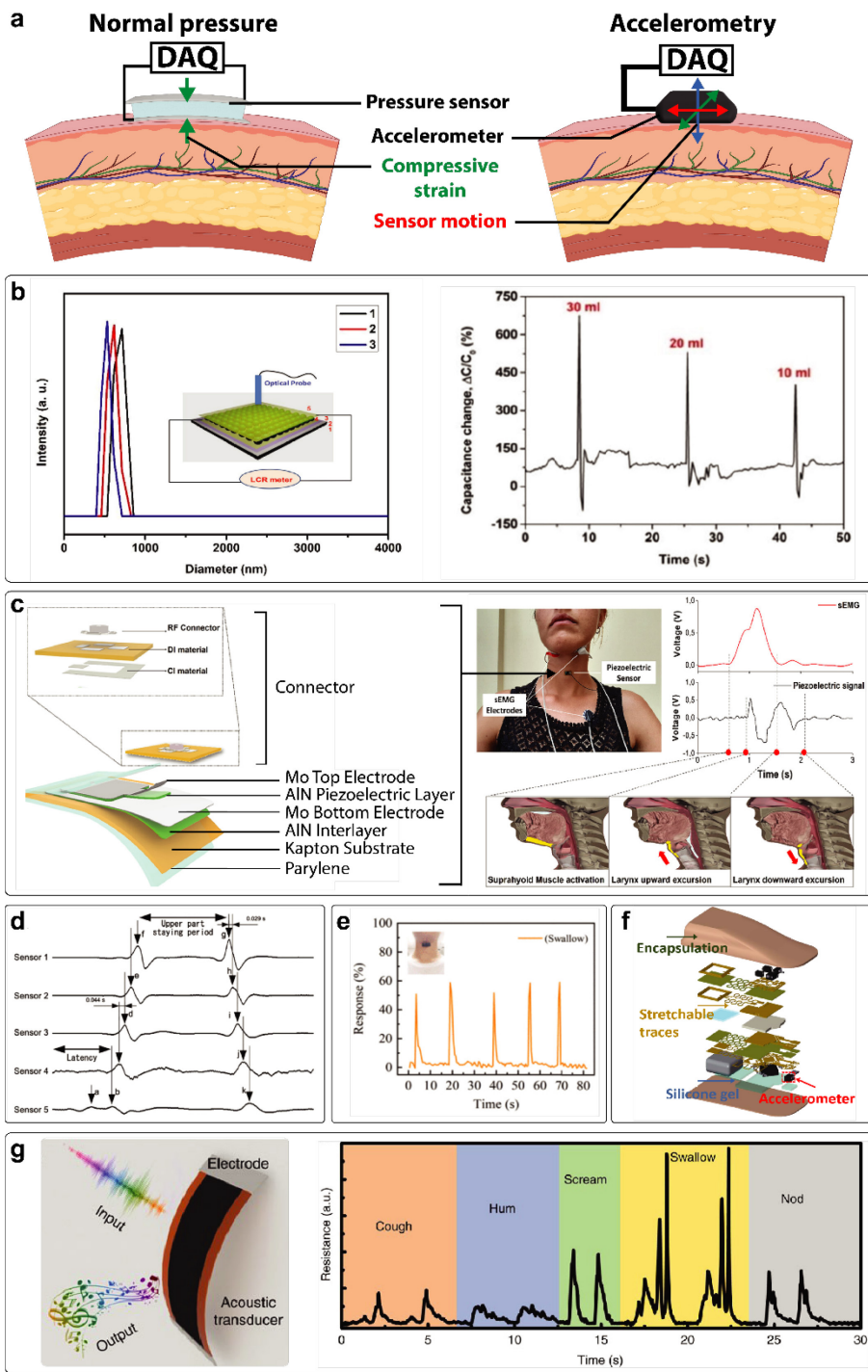


Figure 4: Overview of materials-based pressure sensors and accelerometric sensors applied in swallowing examination. **a**, Typical epidermal pressure sensor reacting to compression caused by skin bending (left), and a mechano-acoustic/ accelerometric sensor reacting to skin motion and deformation. **b**, Optical response from porosity diameter reduction (left) and capacitive response outputs in swallowing experiments demonstrate sensitivity to the consumed bolus volume (right). **c**, A small profile piezoelectric swallowing pressure sensor based on AlN active material. Sensor outputs shown to correspond with laryngeal motion and muscle activity signals. **d**, Temporal parameters extracted from a piezoelectric array. **e**, Reduction of resistance from pressure exerted during swallowing. **f**, Mechano-acoustic sensor patch based on an IMU and a stretchable circuit geometry providing a non-obtrusive attachment and robust wireless data outputs. **g**, Laser induced graphene acoustic sensor, with distinctive signal outputs for various throat-related activities including swallowing. Panels **b**, **d-f**, reproduced with permission.^{73,152,154,158} Panels **c**, **g**, reproduced under Creative Commons (CC BY) license.^{155,163}

1
2
3
4
5
6
7
8
9
10
11
12
13
14

Table 1: A categorical summary of epidermal swallow sensors enabled by recent developments in stretchable conductors and materials.

1

Sensing Modality	Source	Year	Sensor location	Active Materials	SNR	GF/Sensitivity	Spatial Resolution	Human subject experiments	wireless (y/n)	Sensing Mechanism
EMG	Constantinescu et al., Med. Eng. Phys., 38, 807–812	2016	Side (right) of the chin (targeting the right anterior belly of the digastric muscle)	200 nm Au	6.138	-	One pair of sEMG sensor	Proof-of-concept	N	Biopotential
	Nicholls et al., Second IEEE PerCom Workshop on Pervasive Health Technologies, 413–418	2017	Side (left) along submental muscles	300 nm Au	21.4	-	One pair of sEMG sensor	Proof-of-concept	Y	Biopotential
	Lee et al., Sci. Rep. 7, 1–12	2017	Laterally across submental muscles	300 nm thick gold	21.4	-	One pair of sEMG sensor	Proof-of-concept	Y	Biopotential
	Kim et al., Sci. Adv. 5, 1–10	2019	Sides (left and right) along submental muscles	9 μ m Cu and 500 nm Au	-	-	Two pairs of sEMG sensors and a strain sensor	Proof-of-concept	Y	Biopotential

Sensing Modality	Source	Year	Sensor location	Active Materials	SNR	GF/Sensitivity	Spatial Resolution	Human subject experiments	wireless (y/n)	Sensing Mechanism
Biopotential	Kantarcigil et al., J. Speech, Lang. Hear. Res. 63, 3293–3310	2020	Sides (left and right) along submental muscles	9 μ m Cu and 500 nm Au	20.64	-	Two pairs of sEMG sensors	Cohort Study	Y	Biopotential
	Polat et al., Adv. Sensor Res. 2200060	2023	Laterally across submental muscles	PEDOT:PSS(1)-b-PPEGMEA(6)	-	-	One pair of sEMG sensor	Cohort Study	Y	Biopotential
	Wang et al. Sci. Adv. 6 : eabd0996	2020	Multi electrode array placed on the neck and upper chest	100 nm Au	-	-	16 channel sEMG patch	Proof-of-concept	N	Biopotential
Strain	Roh et al., ACS Nano 9, 6252–6261	2015	Medially and horizontally near laryngeal prominence (by inspection)	SWCNTs embedded in PEDOT:PSS/PU complex	-	~136.7 for 2.1% strain	One strain sensor	Proof-of-concept	N	Piezoresistive
	Hwang et al., ACS Nano 9, 8801–8810	2015	Medially and horizontally near laryngeal prominence	AgNWs embedded in PEDOT:PSS/PU complex	-	~12.4 for 2% strain; ~1 for 10–60%	One strain sensor	Proof-of-concept	N	Piezoresistive

Sensing Modality	Source	Year	Sensor location	Active Materials	SNR	GF/Sensitivity	Spatial Resolution	Human subject experiments	wireless (y/n)	Sensing Mechanism
			(by inspection)							
	Zhu et al., New J. Chem. 41, 4950–4958	2017	Medially and horizontally near laryngeal prominence (by inspection)	CuNWs and WGP	-	~175,000 for 2.5% strain	One strain sensor	Proof-of-concept	N	Piezoresistive
	Ramirez et al., ACS Nano 12, 5913–5922	2018	Horizontally side submental muscles	PdNIs on graphene	-	~1 for 0.02% strain	One pair of sEMG sensor and one strain sensor	Cohort Study	N	Piezoresistive
	Polat et al., ACS Appl. Nano Mater. 4, 8126–8134	2021	Medially and horizontally near laryngeal prominence	AuNIs/graphene/ PEDOT:PSS("dough")	-	~17.5 for 0.001% strain	One pair of sEMG sensor and one strain sensor	Proof-of-concept	N	Piezoresistive
	Huang et al., Smart Mater. Struct. 27,	2018	Medially and horizontally below laryngeal prominence (by inspection)	GNPs and CB/SWCNTs	-	~2 for 2.5% strain	One strain sensor	Proof-of-concept	N	Piezoresistive

Sensing Modality	Source	Year	Sensor location	Active Materials	SNR	GF/Sensitivity	Spatial Resolution	Human subject experiments	wireless (y/n)	Sensing Mechanism
	Zang et al., Biomed. Phys. Eng. Express 5,	2019	Medially and horizontally near laryngeal prominence (by inspection)	RGO	-	~250 for 2.5% strain	One strain sensor	Proof-of-concept	N	Piezoresistive
	Zhang et al., Sensors (Switzerland) 17, 1–10	2017	(Unclear)	([EMIM][TFSI]) as the ionic liquid (IL)	-	~560 for 2% strain	One strain sensor	Proof-of-concept	N	Piezoresistive
	Sun et al., Chem. Eng. J. 382, 122832	2020	Medially and horizontally above laryngeal prominence (by inspection)	PAAm-oxCNTs	-	1.5 between 0-250% strain range	One strain sensor	Proof-of-concept	N	Piezoresistive
	Wang et al., J. Mater. Chem. C 9, 575–583	2021	Medially and horizontally near laryngeal prominence (by inspection)	PANI/ANF-PVA	-	~40 for 5%strain	One strain sensor	Proof-of-concept	N	Piezoresistive

Sensing Modality	Source	Year	Sensor location	Active Materials	SNR	GF/Sensitivity	Spatial Resolution	Human subject experiments	wireless (y/n)	Sensing Mechanism
	Xu et al., Colloids Surfaces A Physicochem. Eng. Asp. 636, 128182	2022	Medially and horizontally below laryngeal prominence (by inspection)	MXene nanosheets	-	3.2 between 50-300% strain	One strain sensor	Proof-of-concept	N	Piezoresistive
	Joeng et al. NPG Asia Materials 9, e443	2017	Medially near laryngeal prominence (by inspection)	Encapsulated liquid GaInSn	-	2 for ~30% strain	One strain sensor	Proof-of-concept	Y	Piezoresistive
	Wang et al., Adv. Funct. Mater.	2021	Medially and vertically over laryngeal prominence (by inspection)	RGO and CNT	-	7.2 for 0-60% strain; 89 for 60-120%	One strain sensor	Proof-of-concept	N	Piezoresistive
	Kim et al., Sci. Adv. 5, 1–10	2019	Medially and vertically above laryngeal prominence	Patterened Velostat, 3M	-		Two pairs of sEMG and one strain sensor	Proof-of-concept	Y	Piezoresistive

Sensing Modality	Source	Year	Sensor location	Active Materials	SNR	GF/Sensitivity	Spatial Resolution	Human subject experiments	wireless (y/n)	Sensing Mechanism
			(by inspection)							
	Polat et al., Adv. Sensor Res. 2200060	2023	Medially and horizontally near laryngeal prominence	AuNIs/graphene/PEDOT:PSS("dough")	-	~17.5 for 0.001% strain	One pair of sEMG sensor and one strain sensor	Cohort Study	Y	Piezoresistive
	Zhang et al. Adv. Electron. Mater. 5, 1900285	2019	Medially and horizontally near laryngeal prominence (by inspection)	MXene/ PVA Hydrogel	-	~0.4 for 200% strain	One strain sensor	Proof-of-concept	N	Capacitive
Pressure	Kou et al., Sci. Rep. 9, 1–7	2019	Medially near laryngeal prominence (by inspection)	NH4HCO3/Gr	-	0.12 kPa^-1 between 0-10 kPa	One pressure sensor	Proof-of-concept	Y	Capacitive
	Xia et al., Adv. Mater. Technol. 5, 1–8	2020	Medially below laryngeal prominence (by inspection)	NIPAm/Bis/AAc	-	10.1 kPa^-1 for 2-40 Pa and 1.1 kPa^-1 for 40-110 Pa	One pressure sensor	Proof-of-concept	Y	Capacitive

Sensing Modality	Source	Year	Sensor location	Active Materials	SNR	GF/Sensitivity	Spatial Resolution	Human subject experiments	wireless (y/n)	Sensing Mechanism
	Maeda et al., IEEE 3rd Glob. Conf. Life Sci. Technol. 315–316	2021	Medially near laryngeal prominence	hetero-core fiber optic	-	-	One pressure sensor	Proof-of-concept	N	Optical
	Iizuka et al., J. Physiol. Sci. 68, 837–846	2018	Medially above (0.5–1.0 cm) the laryngeal prominence	PVDF	~75–100	-	Five pressure sensors	Proof-of-concept	N	Piezoelectric
	Natta et al., ACS Sensors 6, 1761–1769	2021	Medially above laryngeal prominence (by inspection)	AlN	-	0.025 V/N	One pair of sEMG sensor and one pressure sensor	Cohort Study	Y	Piezoelectric
	Lee et al., Polymers (Basel). 13	2021	Medially near laryngeal prominence (by inspection)	Au(Phen)Cl ₂ + ion with Au	-	1.5 x e ⁻⁶ mV/kPa	One pressure sensor	Proof-of-concept	N	Ionic polymer–metal composite
	Guan et al.	2021	Medially near laryngeal prominence (by inspection)	MoSe ₂ /MWNT		0.24-0.35 kPa ⁻¹	One pressure sensor	Proof-of-concept	N	Piezoresistive

Sensing Modality	Source	Year	Sensor location	Active Materials	SNR	GF/Sensitivity	Spatial Resolution	Human subject experiments	wireless (y/n)	Sensing Mechanism
	Park et al. Adv. Mater. 29, 1702308	2017	Medially below laryngeal prominence (by inspection)	PZT		0.018 kPa ⁻¹	One pressure sensor	Proof-of-concept	Y	Piezoelectric
Mechano-acoustic	Tao et al., Nat. Commun. 8, 1–8	2017	Medially near laryngeal prominence	Laser-induced graphene	-	31 mV/Pa	One acoustic sensor	Proof-of-concept	N	Resistance
	Lee et al., Nat. Biomed. Eng. 4, 148–158	2020	Over suprasternal notch	N/A	-	-	One IMU sensor	Cohort Study	Y	Motion/ Acceleration
	Kang et al. NPJ Digital Med.	2022	Over suprasternal notch/ over laryngeal prominence	N/A	-	-	Two IMU Sensors	Cohort Study	Y	Motion/ Acceleration

1

2